Behind the Beam Stop and Beyond:
Measuring the Microstructure of Technologically Important Materials using Quantitative Small-Angle Scattering

53rd Annual Denver X-ray Conference, 2-6 August 2004, Sheraton Steamboat Springs Resort, Colorado

Pete R. Jemian

University Of Illinois at Urbana-Champaign
UNICAT, Advanced Photon Source
Argonne National Laboratory

This presentation may be viewed at
http://www.uni.aps.anl.gov/~jemian/docs/dxc-2004-08-03-jemian.htm

The UNICAT facility at the Advanced Photon Source (APS) is supported by the U.S. DOE under Award No. DEFG02-91ER45439, through the Frederick Seitz Materials Research Laboratory at the University of Illinois at Urbana-Champaign, the Oak Ridge National Laboratory (U.S. DOE contract DE-AC05-00OR22725 with UT-Battelle LLC), the National Institute of Standards and Technology (U.S. Department of Commerce) and UOP LLC. The APS is supported by the U.S. DOE, Basic Energy Sciences, Office of Science under contract No. W-31-109-ENG-38.

Why small-angle scattering?

Premier method for size characterization of nanoscale density inhomogeneities

- Why quantitative SAXS?
  - Determine volume fraction and number density

Outline

- Small-Angle Scattering Primer
- Quantitative Small-Angle Scattering
- Instrumentation
- Examples
- Summary

How might I summarize Small-Angle Scattering?

- Studies complement other methods
- Applicable to wide variety of technologically important materials
- Indirect measure of size, amount, or shape
- Easy experiment, harder analysis
- Sample in transmission, $t=1/\mu$
- Monochromatic radiation ($\Delta\lambda/\lambda$ up to 25% is acceptable)

What can be learned from a Small-Angle Scattering Experiment?

- Size of scatterer
- Amount of scatterers
- Polydispersity
- Distribution of scatterers
- Shape of scatterers
- Morphology of scatterers
- Composition of scatterers

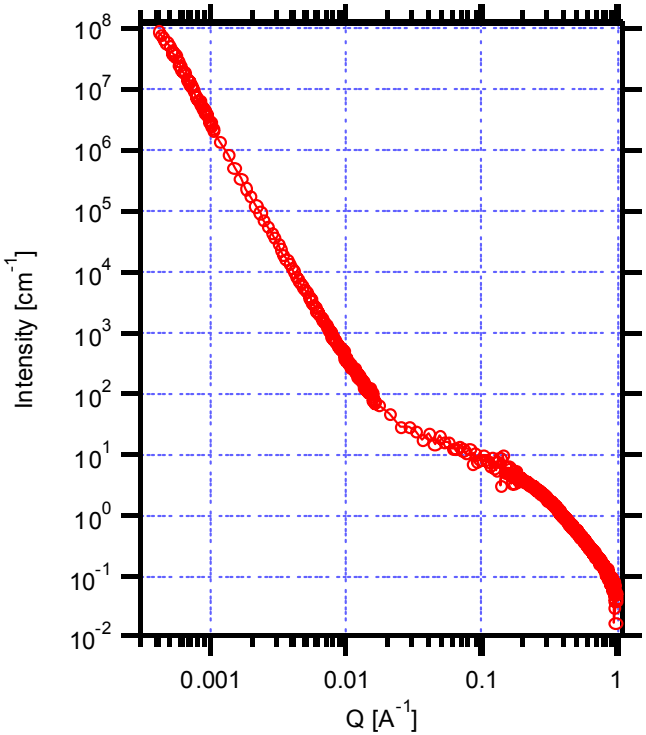

•There is *strong* dependence between some of these terms.
•SAS experiments, *complemented by other measurements*, can yield rich information about the microstructure.

What types of materials can be investigated with Small-Angle Scattering?

- Materials science:
  - PS spheres: diameter & polydispersity
  - Depletion restabilization of colloidal silica
  - Microstructure of porous silica precursor bodies
  - Yttria-stabilized zirconia
  - Paint pigment
  - Colloidal silica
- Human medicine
  - Toughening of PMMA bone cement
- Environmental science
  - Yucca Mountain Groundwater Colloids
- Anomalous scattering contrast variation
  - Silicon Nitride for gas turbine engines
  - Stability of modified Fe9Cr1Mo Steel at high service temperatures

- Samples with nanoscale density inhomogeneities
- Samples that can transmit > few percent of beam

Need for complementary methods

The richness of an integrated approach to materials characterization is dependent on the availability of complementary methods.

The more you know
the more you can learn.

Example: M_2C in AF1410 Steel

Complementary Methods:
XRD, TEM, AP/FIM, SANS,
mechanical properties,
thermodynamics calculations

SANS results bridged gap between
TEM & AP/FIM size data
Also provided new information of
volume fraction and number density

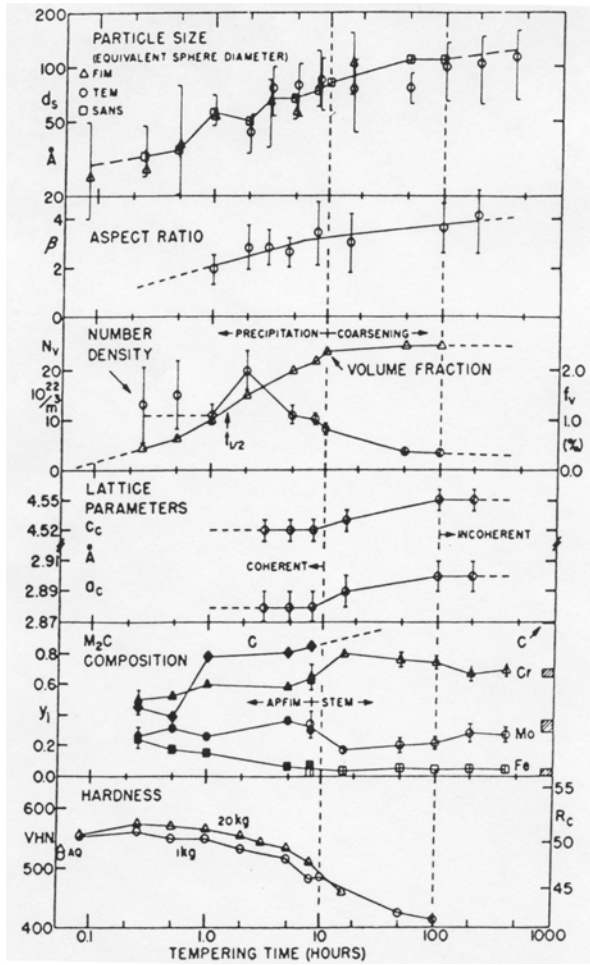

J.S. Montgomery, 1990,
Ph. D. Thesis, Northwestern University.

A.J. Allen, D. Gavillet, and J.R. Weertman;
***Acta Metall* 41** (1993) 1869-1884.

Innovations in Ultrahigh-Strength Steel Technology,
edited by G.B. Olson, M. Azrin, and E. S. Wright
Proceedings of the 34th Sagamore Conference,
August 30 - September 3, 1987, Lake George, NY, 1987

Origin of scattering

- Scattering is due to inhomogeneities in scattering length density, ρ
- Scatterers are
  - Homogeneous
  - Dilute (non-interacting)
  - Randomly dispersed
  - Same morphology
  - Same contrast, $|\Delta\rho|^2$

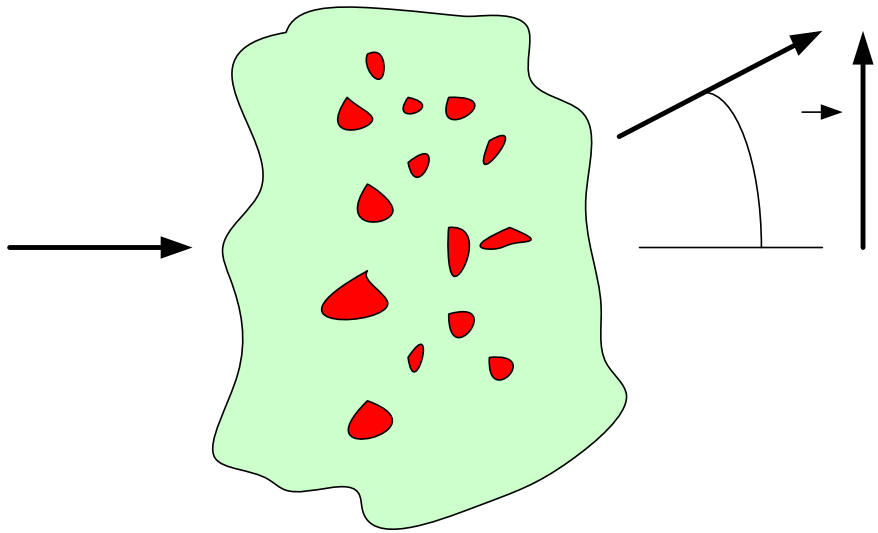

$$\frac{d\Sigma}{d\Omega}(\vec{Q}) = \left| V_p^{-1} \int_{V_p^{-1}} \rho(\vec{r})\, e^{-\vec{Q}\cdot\vec{r}}\; d^3\vec{r} \right|^2$$

$$Q = \frac{4\pi}{\lambda}\sin\theta$$

Basic measures from a Small-Angle Scattering experiment

Guinier law $$\lim_{Q\to 0} I(Q) = I(0)\exp\left(-\frac{1}{3}R_G^2 Q^2\right)$$

$$Q_{\max} R_G < 1.2$$

Porod law $$\lim_{Q\to \infty} I(Q) = 2\pi S_V \left|\Delta\rho\right|^2 Q^{-4}$$

$$Q_{\min} D > 3$$

invariant $$2\pi^2 V_V \left(1 - V_V\right)\left|\Delta\rho\right|^2 = \int_0^\infty Q^2 I(Q)\, dQ$$

Outline

- Small-Angle Scattering Primer
- Quantitative Small-Angle Scattering
- Instrumentation
- Examples
- Summary

Advantages of Quantitative SAS

- Sampling volume large compared to features investigated: *Statistically Significant Sampling*
  - Sample volume typically 10^{-12} - 10^{-10} m^3
  - Scatterer size typically 10^{-9} - 10^{-6} m
  - 10^3 - 10^{13} scatterers in a single sample volume
- SAS probes through bulk material, not limited to surface or open porosity
- X-ray or neutron radiation sources can probe optically opaque substances
- Can separate different components in multi-component system (in some cases)

Information Obtained from Quantitative Small-Angle Scattering

volume fraction

$$V_V = \sum_i f_i(D)\Delta D_i$$

number density

$$N_V = \sum_i \frac{f_i(D)\Delta D_i}{(\pi/6)D_i^3}$$

Radius of gyration

$$R_G = \sqrt{\langle r^8 \rangle / \langle r^6 \rangle}$$

specific surface

$$S_V = 6\sum_i f_i(D)\frac{\Delta D_i}{D_i}$$

mean spacing

$$\Lambda = (N_V)^{-1/3}$$

	volume-weighted	number-weighted
mean diameter	$\overline{D}_V = V_V^{-1}\left[\sum_i D_i f_i(D)\Delta D_i\right]$	$\overline{D}_N = N_V^{-1}\left[\sum_i D_i \frac{f_i(D)\Delta D_i}{(\pi/6)D_i^3}\right]$
standard deviation	$\sigma(\overline{D}_V) = \sqrt{V_V^{-1}\left[\sum_i D_i^2 f_i(D)\Delta D_i\right] - (\overline{D}_V)^2}$	$\sigma(\overline{D}_N) = \sqrt{N_V^{-1}\left[\sum_i D_i^2 \frac{f_i(D)\Delta D_i}{(\pi/6)D_i^3}\right] - (\overline{D}_N)^2}$

Absolute SAS Cross-Section $d\Sigma/d\Omega$

J Appl Cryst **5** (1972) 315-324, **16** (1983) 473-478
Acta Metall Mater **39**.11 (1991) 2477-2487

$$I(Q) = I_0 \, \Omega \, t \, e^{-\mu t} \, \frac{d\Sigma}{d\Omega}(Q)$$

$I(Q)$: intensity, arbitrary units

I_0 : apparent source intensity, arbitrary units

Ω : solid angle subtended by detector

t : sample thickness

μ : absorption coefficient

$d\Sigma(Q)/d\Omega$: differential scattering cross-section per unit volume per unit solid angle

Methods to obtain $d\Sigma/d\Omega$

Comparison of USAXS: Direct Intensity Scaling

- Direct measurement of all parameters
- Calibration against secondary standard

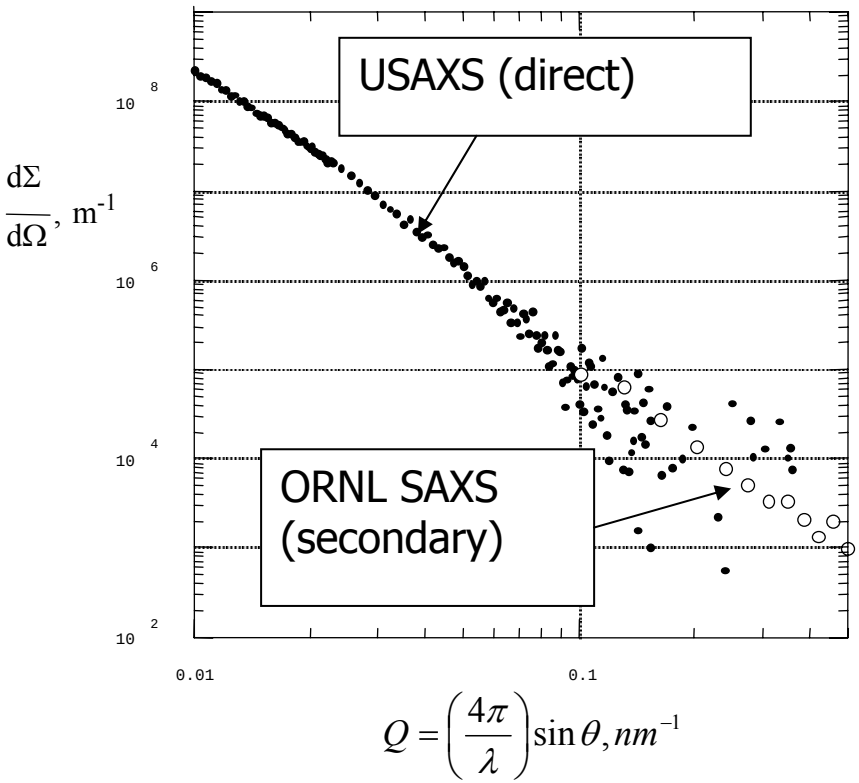

Jemian, Ph.D. Thesis, 1990, Northwestern

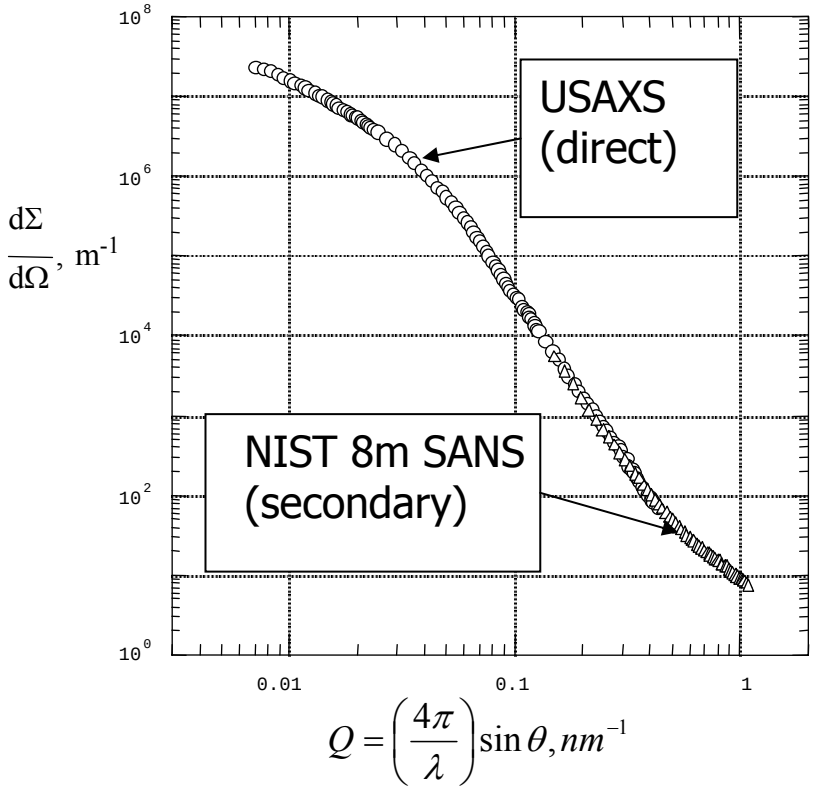

Long, et al., *J Appl Cryst* **23**.6 (1990) 535

Size Distribution Determination

$$\frac{d\Sigma}{d\Omega}(Q) = \int_0^\infty \left|\Delta\rho\, F(Q,r)\, V(r)\right|^2 N(r)\, dr$$

$$\frac{d\Sigma}{d\Omega}(Q) = \left|\Delta\rho\right|^2 \int_0^\infty \left|F(Q,r)\right|^2 V(r) f(r)\, dr$$

Solve for $f(r)\, dr$ by a regularization method such as:

- enforcing only positive values of $f(r)\, dr$
- maximizing smoothness of $f(r)\, dr$

Spheres: $F(Q,r) = 3(Qr)^{-3}\left[\sin(Qr) - (Qr)\cos(Qr)\right]$

–*Acta Metall Mater* **39**.11 (1991) 2477-2487

MaxEnt size distribution

Rewrite as linear inverse problem

$$\frac{d\Sigma}{d\Omega}(Q) = |\Delta\rho|^2 \int_0^\infty |F(Q,r)|^2 V(r) f(r)\, dr \longrightarrow \vec{I} = \underline{G}\vec{f}$$

Fit the experimental data (subject to uncertainties)

$$\chi^2 = \sum \left(\frac{I - \underline{G} f}{\sigma} \right)^2$$

Also maximize configurational entropy of solution

$$S = -\sum f \log(f / b)$$

J. Skilling and R.K. Bryan; ***Mon Not R Astr Soc* 211** (1984) 111-124.
J.A. Potton, G.J. Daniell, and B.D. Rainford; ***J Appl Cryst* 21** (1988) 891-897, 663-668.

What can we do for more complex samples, such as γ' precipitation in Waspaloy™ ?

Gerhardtl, private communications, 2000

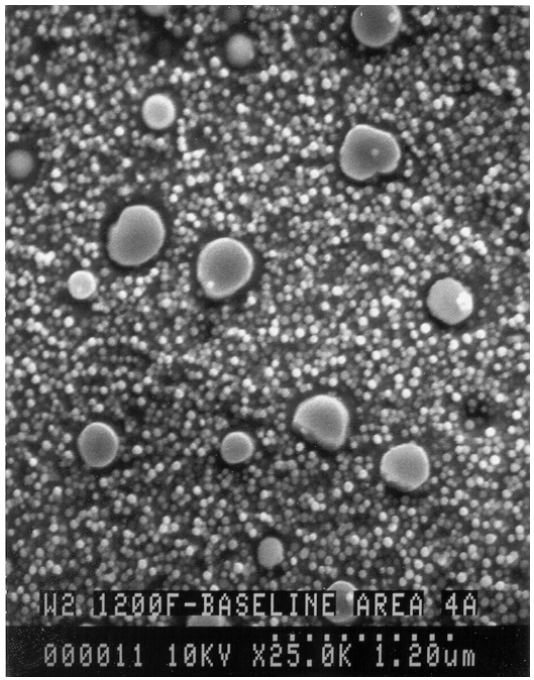

base microstructure

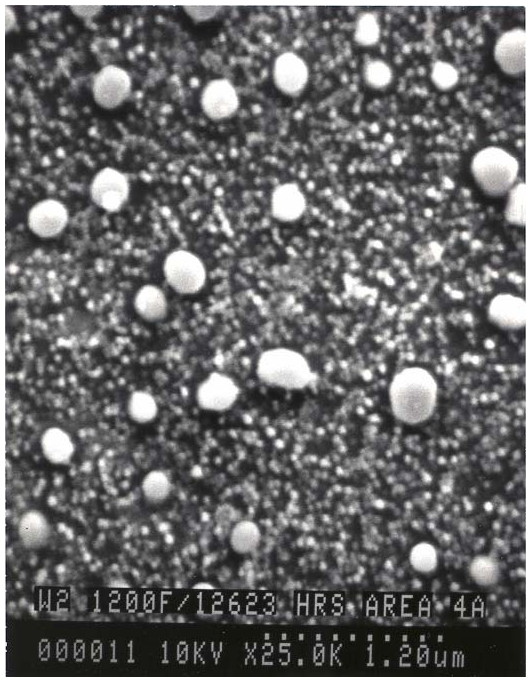

12623 h, 1200° F

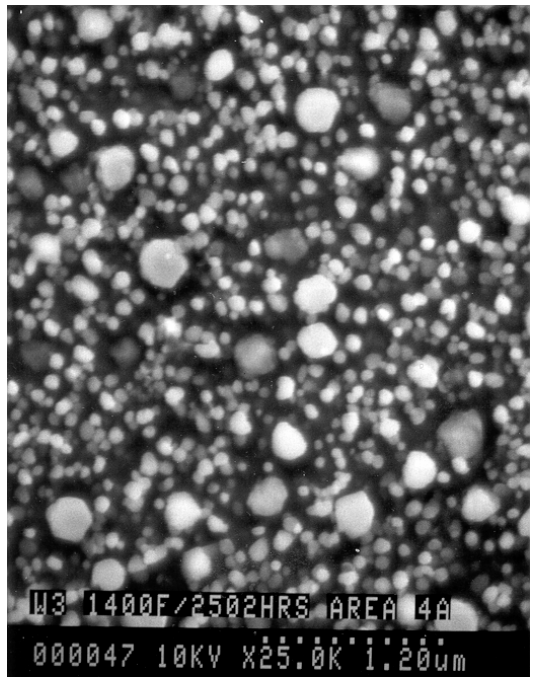

2502 h, 1400 ° F

Simple contrast variation example

When the monster came, Lola, like the peppered moth and the arctic hare, remained motionless and undetected. Harold, of course, was immediately devoured.

When the monster came, Lola, like the peppered moth and the arctic hare, remained motionless and undetected. Harold, of course, was immediately devoured.

Contrast Variation Methods

- Needed when more than one type of scatterer is present
- Vary $|\Delta\rho|^2$ of one type, holding others constant

- Anomalous scattering (X-ray & neutron)
- Isotope substitution (neutron)
- Isomorphous replacement
- Magnetic scattering (neutron)
- Concentration variation (X-ray & neutron)
- ...

Anomalous Small-Angle X-ray Scattering

- Why anomalous SAXS?
  - Element-specific contrast variation
  - Use to separate population distributions of scatterers
- Will ASAXS solve every problem?
  - Not even close
  - The easy problems are already taken

Calculated *f'(E)* and *f''(E)*

Anomalous dispersion terms of
Yb in SN-88 near the Yb L_{III} edge (8.939 keV)

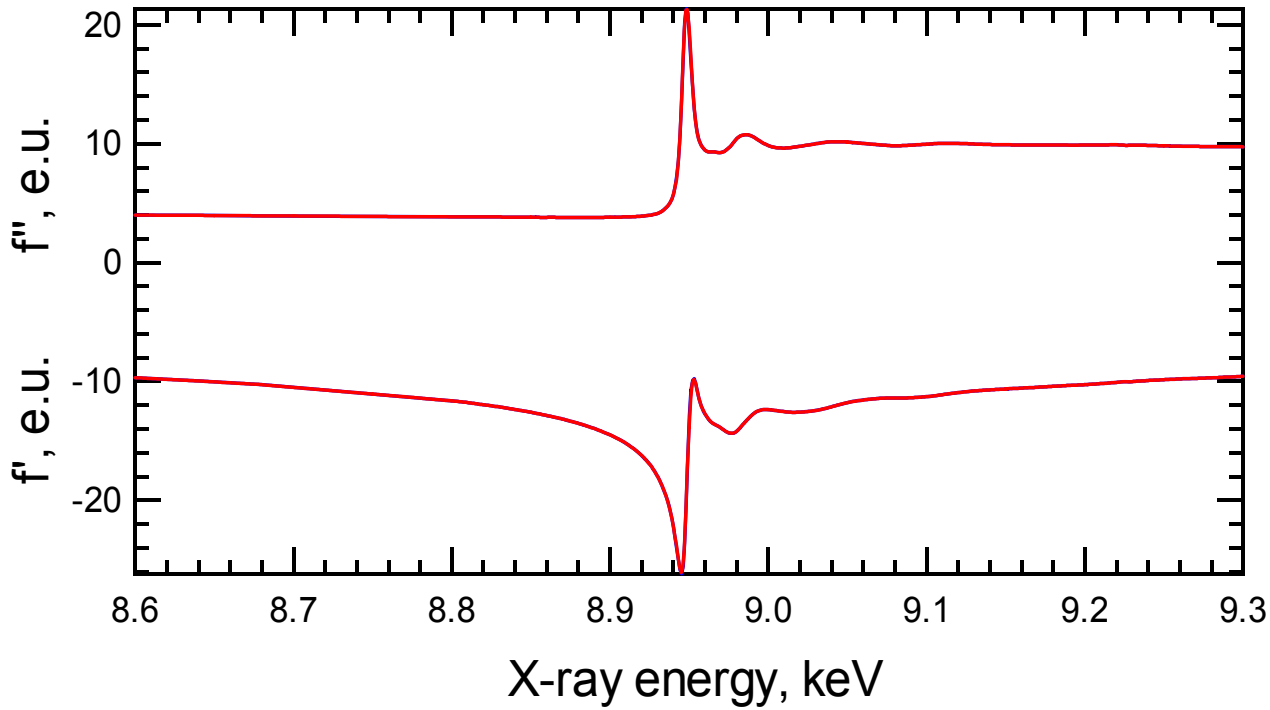

Calculation of *f'(E)* and *f''(E)*

- The anomalous dispersion terms are calculated from the absorption spectrum:
  - *Z Phys* **48** (1928) 174-179, *J Appl Cryst* **17** (1984) 344-351

Beer's Law $$\frac{I}{I_0} = \exp\left[-\mu_l(E)t\right]$$

optical theorem $$f''(E) = \frac{E}{2r_e ch}\frac{A}{N_A}\frac{\mu_l(E)}{\rho_m} = \frac{E}{2r_e ch}\frac{A}{N_A}\mu_m(E)$$

Kramers-Kronig integral $$f'(E) = \frac{2}{\pi}\int_0^\infty f''(\varepsilon)\frac{\varepsilon}{E^2 - \varepsilon^2}d\varepsilon$$

ASAXS Analytical Method

- Absorption spectrum
  - Energy selection
  - Determine anomalous scattering factors
  - Calculate scattering contrasts
- SAXS measurements
  - Sample and blank at each energy
  - Calculate transmission
  - Subtract blank
  - Apply corrections (e.g., desmearing)
  - Solve for size distribution
- ASAXS analysis
  - Extract size distribution for each scatterer using contrast gradient method
  - Assess integral, mode, mean, standard deviation, etc. for each size distribution

A-USAXS, the basics

scattering vector magnitude

$$Q = (4\pi/\lambda)\sin\theta$$

intensity of scattering

$$I(Q) = \frac{d\Sigma}{d\Omega}(Q,E) = \sum_k \left|\Delta\rho_k(E)\right|^2 \int_0^\infty N_k(D)V^2(D)\left|F(Q,D)\right|^2 dD$$

intensity, simplified

$$I(Q,E) = \int_0^\infty \varphi(D,E)\, G(Q,D)\, dD$$

Solve for $\varphi(D,E)$ with MaxEnt, regularization, or some other constrained method.
For example, *J Appl Cryst* **21**.6 (1988) 663-668.

Use scattering contrast to separate *f(D)* for each population

$$\varphi(D,E) = \left|\Delta\rho_{disilicate}(E)\right|^2 f_{disilicate}(D) + \left|\Delta\rho_{void}\right|^2 f_{void}(D)$$

determination of creep cavity population

$$f_{creep\,cavities}(D) = f_{void,gage}(D) - f_{void,grip}(D)$$

Necessary Measurements

- *a priori* information
  - Sample composition
  - TEM/STEM/AFM/AP-FIM
  - XRD
  - Porosimetry
  - Gas adsorption
  - …
- Sample thickness
- Sample uniformity
- Sample absorption spectrum
- Instrument absorption spectrum
- Sample (+instrument) SAXS
- Instrument SAXS profile
- Absolute SAXS cross-section $d\Sigma/d\Omega$

Sample Uniformity Measurement

- Illuminated area must be representative of sample
- Sample thickness must be uniform
- No pinholes
- Sample positioning must be *precise* and *reproducible*
  - How precise?
    - Depends on beam size & sample uniformity
    - Precision (step size) ~ 20 μm
    - Reproducibility < 50 μm
  - Achieve with a X-Y translation stage
- Verify using *radiography* and *USAXS imaging*

Absorption Spectrum Measurement

- Use to determine position of absorption edge
- Calibrate energy for experiment
- Derive anomalous dispersion corrections

X-ray absorption spectrum of SN-88 near the Yb L_{III} edge (8.939 keV)

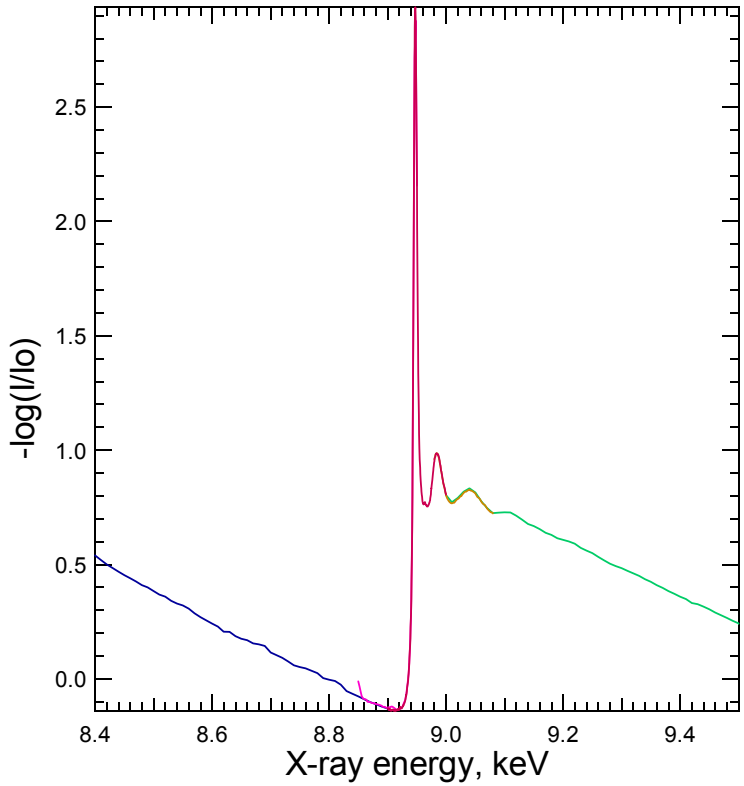

ASAXS Energy Selection Criteria

- Maximize contrast change of target population, work near absorption edge
- Minimize the energy range to be covered, 200-300 eV sufficient
- Avoid X-ray fluorescence, stay below absorption edge
- Avoid Resonant Raman Scattering, stay away from absorption
- Consider monochromator energy tails, measure absorption spectrum from SAXS sample!
- Maximize the number of energies
- Use all available beam time

Energy Selection, contrast

Calculate the scattering contrast of the major populations
Choose energies so that $|\Delta\rho(E)|^2$ are evenly-spaced

$$\Delta\rho_k(E) = r_e(E)\sum_Z \Delta c_Z\left[Z + f'_Z(E) + if''_Z(E)\right]$$

X-ray scattering contrast of scatterers in SN-88 near the Yb L_{III} edge

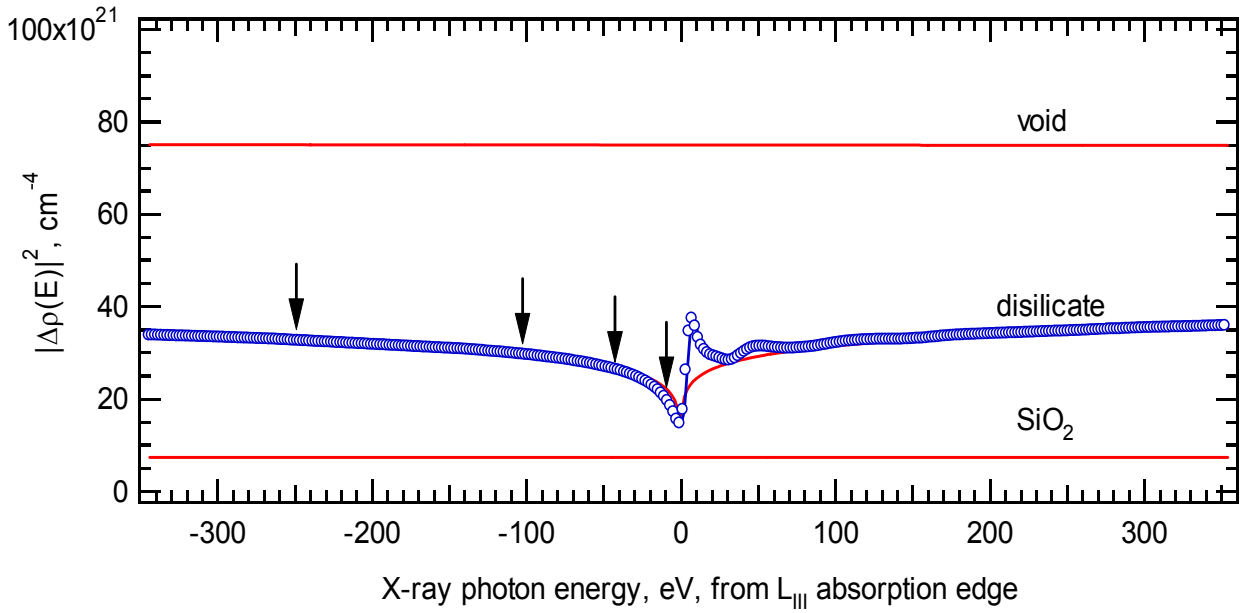

Energy Selection, absorption

- Don't get too ambitious (a.k.a. greedy)
- Stay below the absorption edge
  - No closer than –15 to -25 eV for K edges
  - No closer than –30 to -40 eV for L_{III} edges
- No closer than minimum of absorption spectrum

X-ray absorption spectrum of SN-88 near the Yb L_{III} edge (8.939 keV)

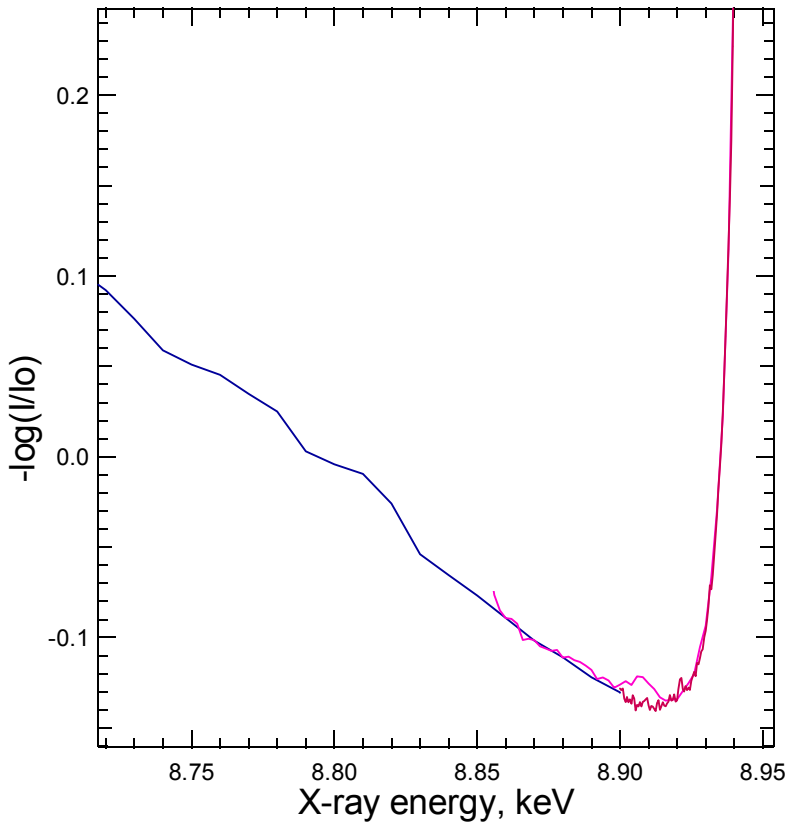

Outline

- Small-Angle Scattering Primer
- Quantitative Small-Angle Scattering
- Instrumentation
- Examples
- Summary

Instrumentation

The trick is to measure an intensity which varies by several decades *very* close to the intense transmitted beam. Must avoid damaging the detector with the transmitted beam!

Designs

- Slit cameras
- Pinhole cameras
- Ultra-Small-Angle (a.k.a, USAS or Bonse-Hart)
- Grazing incidence (reflection, not transmission)

Sources

- X-ray tube
- Rotating anode
- Synchrotron X-ray source
- Reactor
- Pulsed neutron source

APS SAXS instruments

http://small-angle.aps.anl.gov

Nine different small-angle X-ray scattering (SAXS) beam lines are accessible to the APS general user. The combined capabilities of these beam lines span a broad range of reciprocal space and X-ray photon energy allowing for investigations from many disciplines of science including biology, materials science, environmental science, chemistry, medicine, and physics. Coupled with a high data throughput and fast time-resolved measurement capabilities, these instruments enable an efficient use of the high intensity and high brilliance APS X-ray source.

accessible Q range

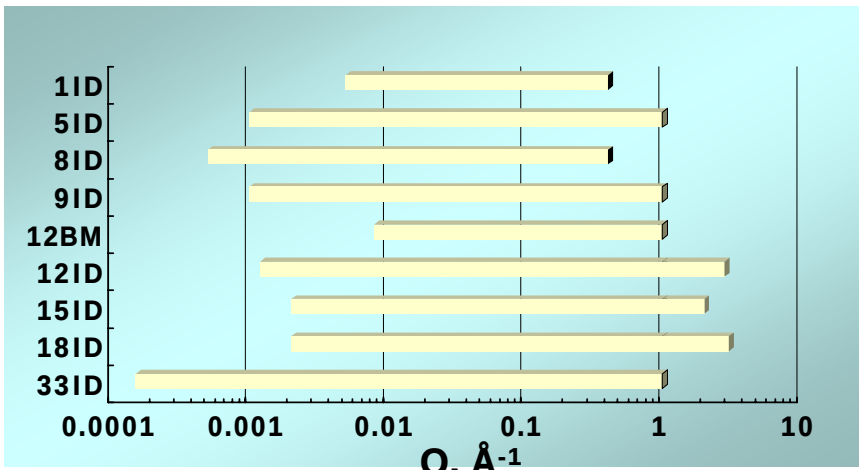

accessible energy range

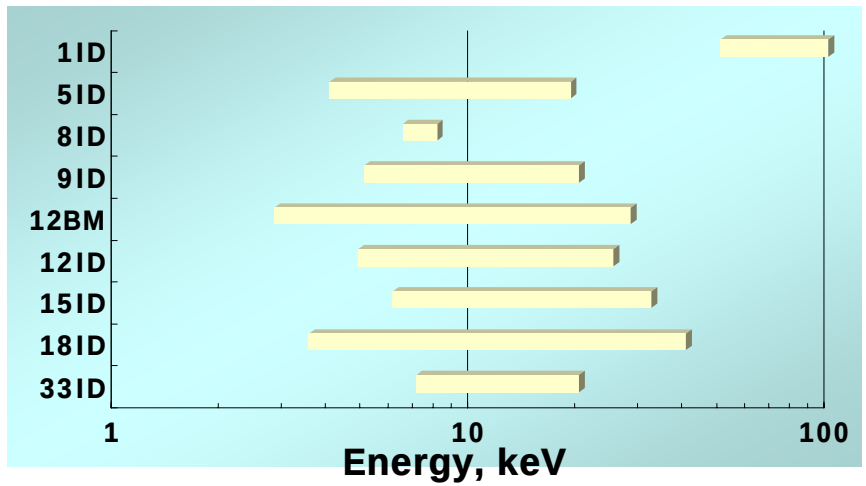

Example pinhole SAXS: BioCAT

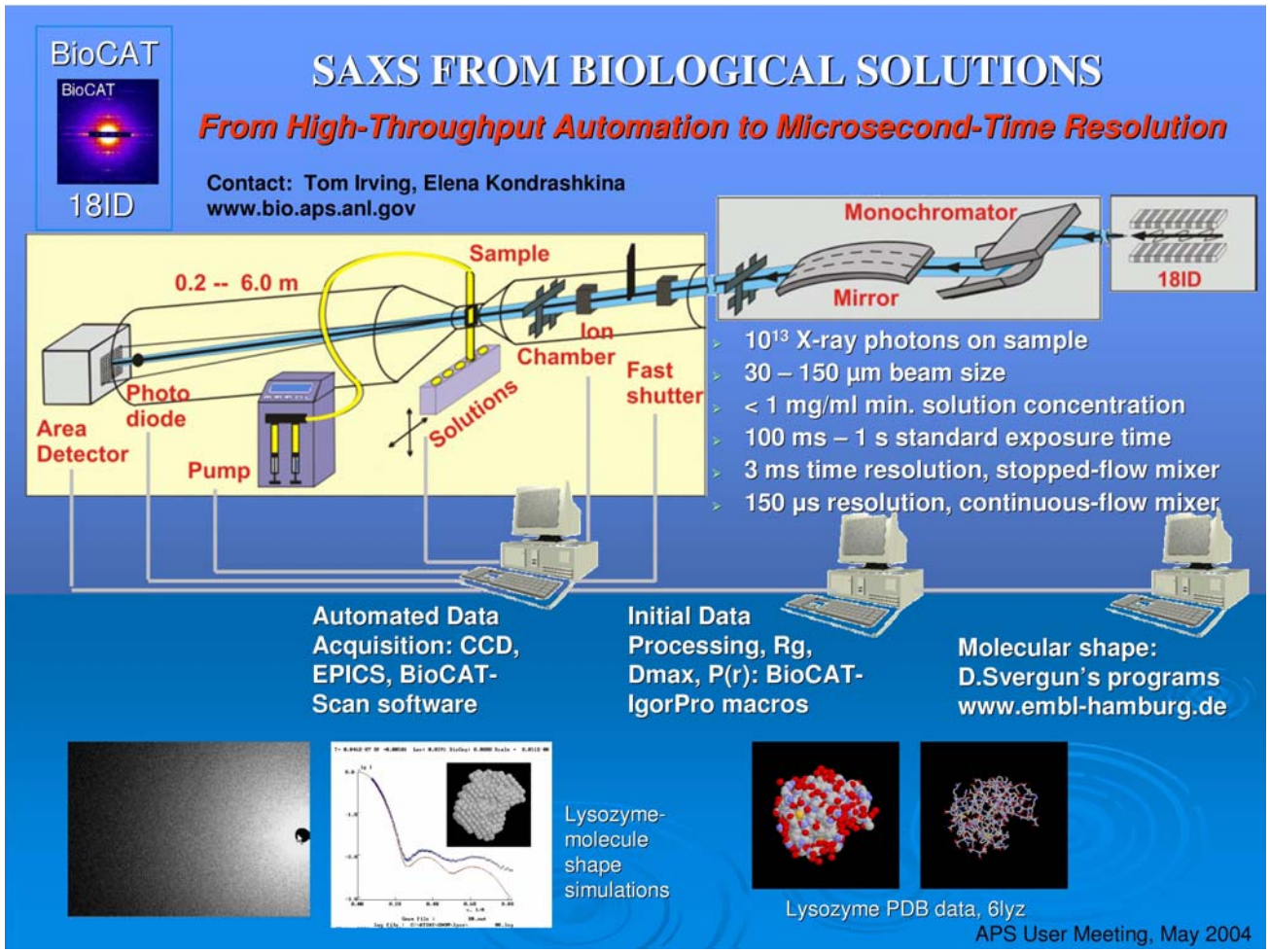

Example pinhole SAXS: 8ID

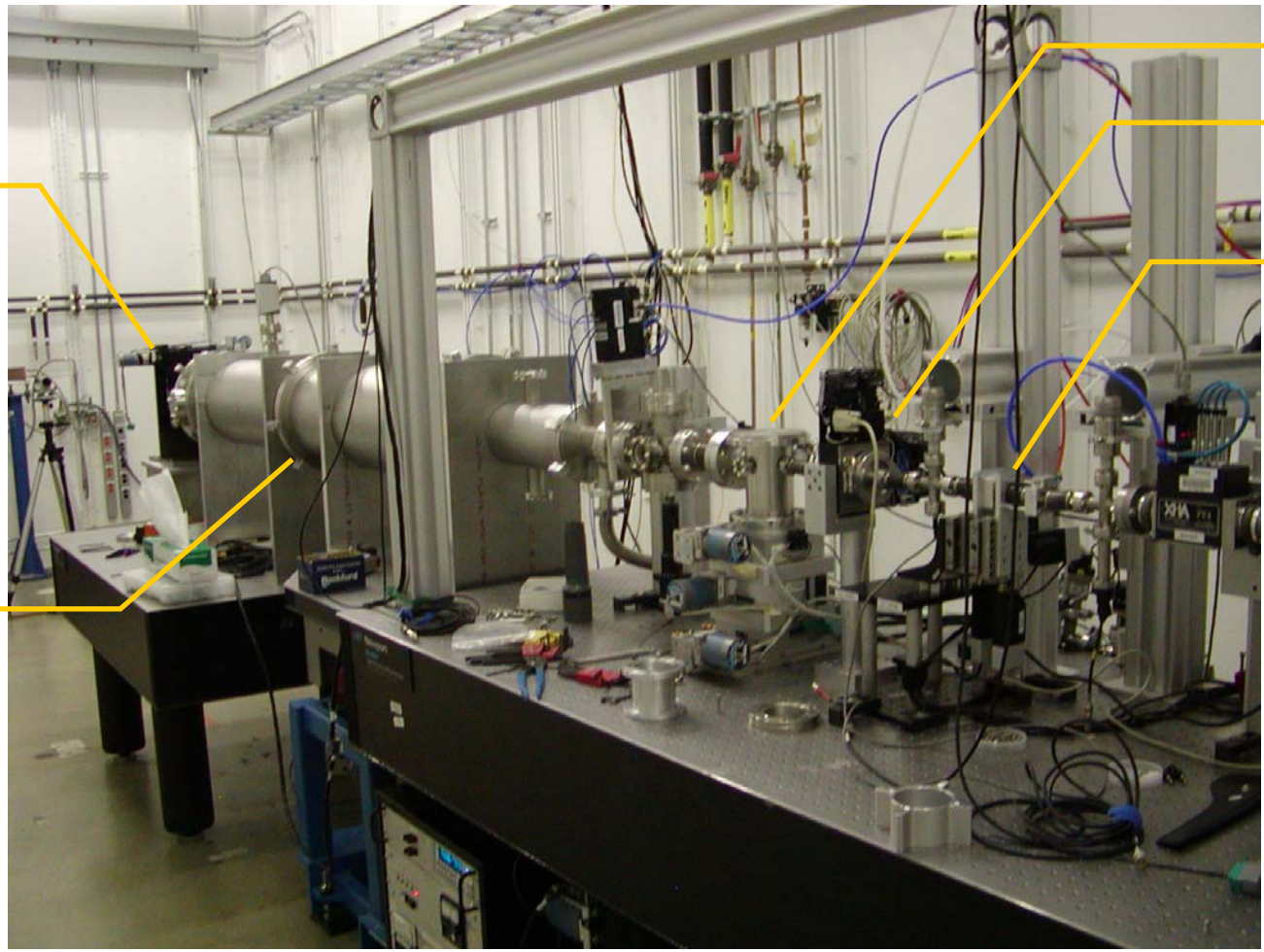

Beam stop limits largest size resolved

Beam stop

- Needed to protect detector
- Limits minimum Q , typical Q_{min}~10^{-3} $Å^{-1}$, (d_{max}~200-600 nm)

$$Q_{\min} d_{\max} \sim 2\pi$$

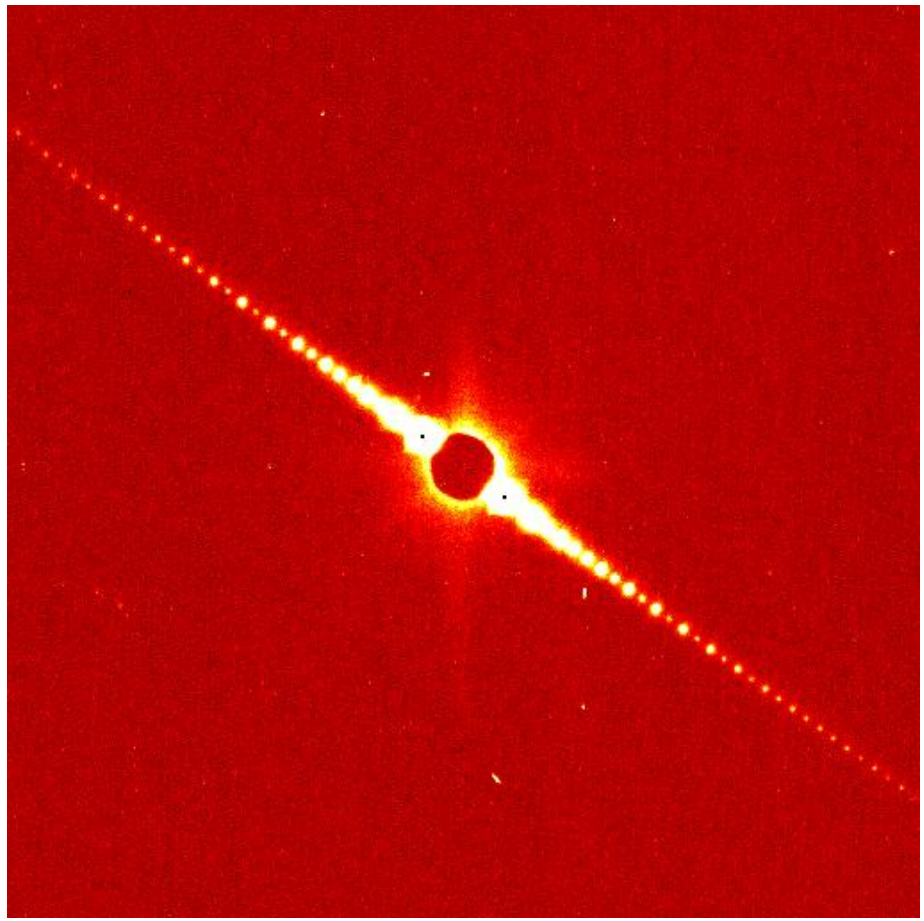

Ultra-Small-Angle X-ray Scattering

- Why Ultra-Small-Angle X-ray Scattering?
  - Resolve scattering from inhomogeneities larger than 100 nm
  - Address the question:
    "What's behind the beam stop?"
- What is different than regular SAXS?
  - Angular collimation by Bragg reflection
  - Shorter instrument
  - No time-resolution

Basic idea of Bragg collimation

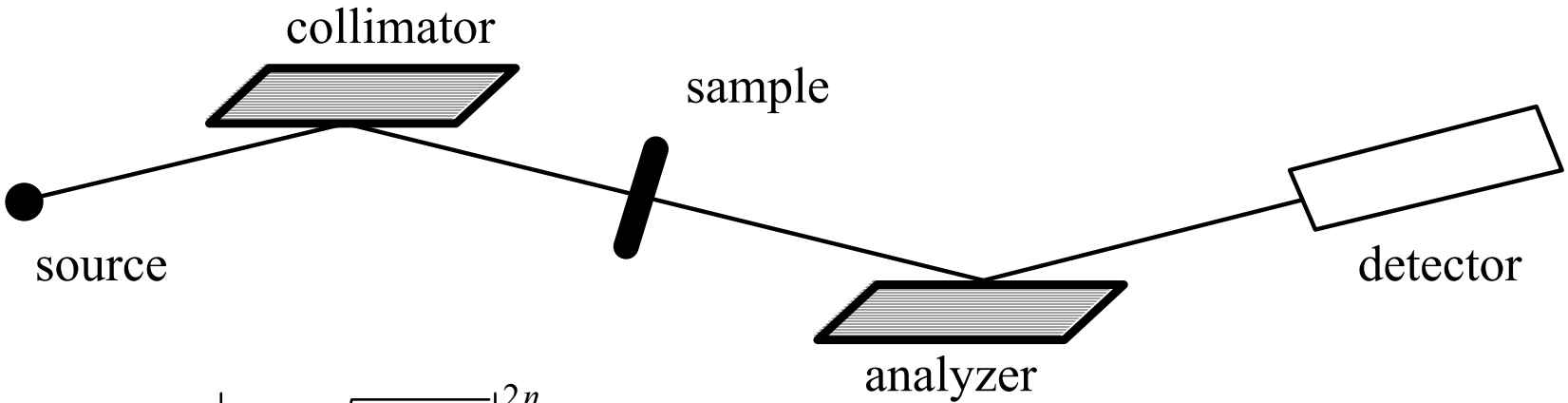

$$D_n(y) = \left| y \pm \sqrt{y^2 - 1} \right|^{2n}$$

$$y = \frac{(1\text{-}m)\, F_0 + 2\, m \left(\theta_B\text{-}\theta\right) \Gamma^{-1} \sin\left(2\theta_B\right)}{2\, T \sqrt{|m|\, F_H\, F_{\overline{H}}}}$$

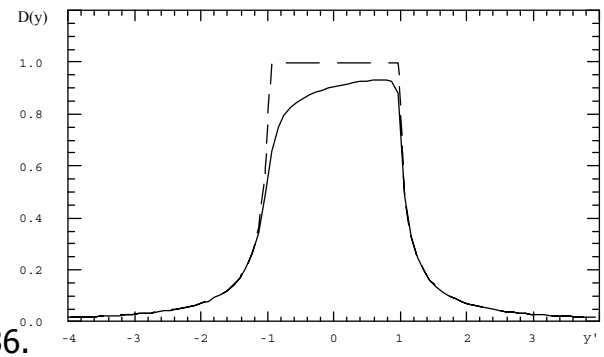

Need at least n=2 before and after sample

Paul Kaesberg, W.W. Beeman, and H.N. Ritland; ***Phys Rev* 78** (1950) 336.
Ulrich Bonse and Michael Hart; ***Appl Phys Lett* 7** (1965) 238-240, ***Z fur Physik* 189** (1966) 151-162.

Pinhole vs USAS

Camera	Pros	Cons
Pinhole	• Simple design • Can use area detector • Time-resolved studies • Adjust collimation with slits • No slit smearing	• $Q_{min} > 0.001$ Å^{-1} • Can't reject fluorescence • Long detector distance needed for high resolution
USAS	• reaches very small Q • compact size • absolute cross-section • rejects fluorescence • examine larger sample volume without compromising resolution	• must use step-scan • must correct for slit collimation • Bragg reflection is background • More complex operation • Adjust collimation by changing crystal optics

Slit-Smearing Geometry

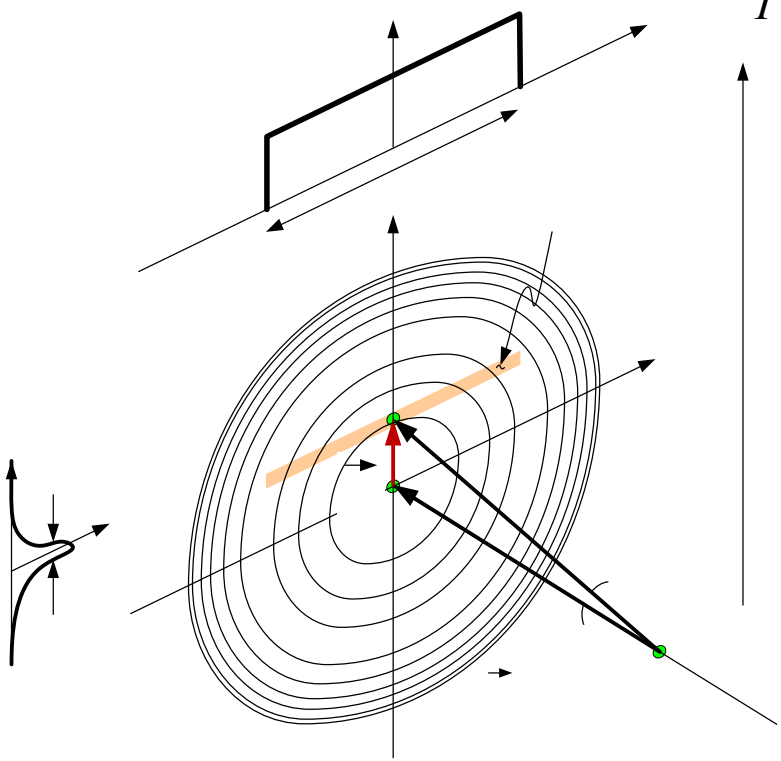

General Collimation Broadening Formula

$$\tilde{I}(Q) = \int_0^\infty P_\lambda(\lambda) \int_{-\infty}^\infty P_w(w) \int_{-\infty}^\infty P_l(l)\, I(Q,\lambda,w,l)\, d\lambda\, dw\, dl$$

Instrumental Collimation Function

$$1 \equiv \int P_x(x)\, dx$$

Rectangular Slit Collimation in USAXS

$$\tilde{I}(Q) = l_0^{-1} \int_0^{l_0} I\left(\sqrt{Q^2 + l^2}\right) dl$$

typical collimation ratio in USAXS

$$w_0 \approx l_0 / 200$$

Desmearing Examples

Waspaloy, measured and corrected

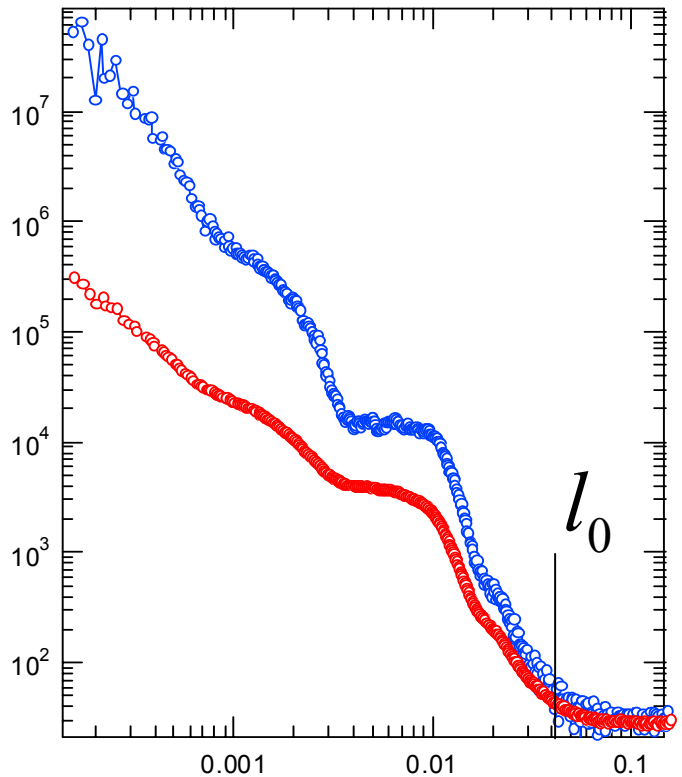

J.A. Lake; ***Acta Cryst* 23** (1967) 191-194.

Silica spheres: 1-D & 2-D USAXS

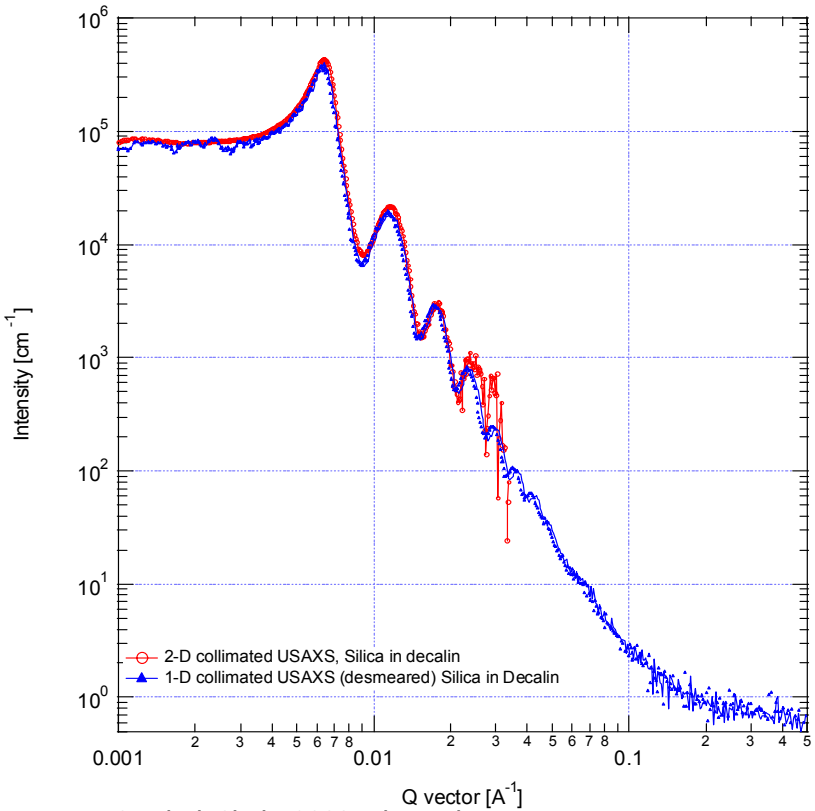

Syed Ali Shah, 2003, Ph.D. Thesis,
University of Illinois at Urbana-Champaign.

UNICAT USAXS Instrument

Versatile USAXS (Bonse-Hart) facility for advanced materials research at APS Beam Line 33ID-D

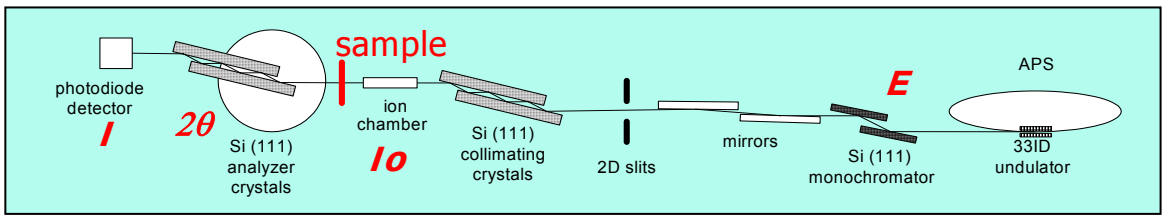

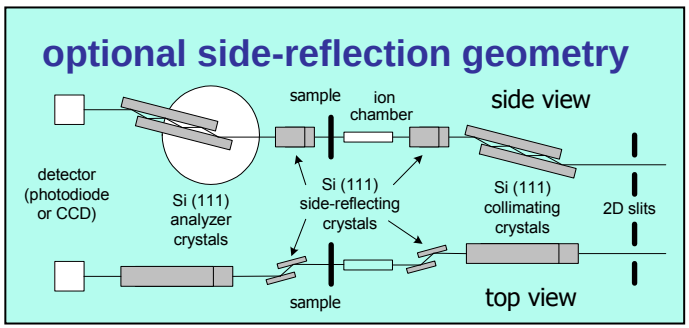

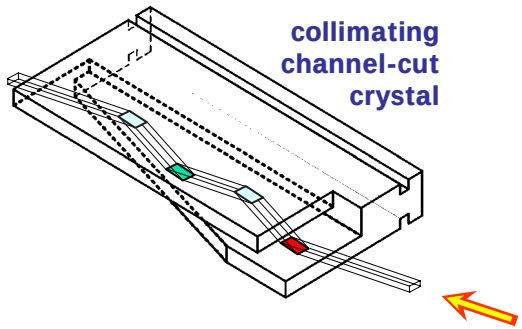

- Q range: 0.00015 ≤ Q, Å^{-1} ≤ 1
- X-ray energy tunability: 7 – 20 keV
- energy resolution: $\Delta E/E \approx 0.00015$
- energy harmonic content < 10^{-6}
- 0.5 x 2 mm^2 beam size, adjustable
- I_0 >10^{12} ph/s (10 keV) delivered to sample
- sample in air (ca. 1/4 m from detector)
- automatic sample changer/translation stage
- absolute determination of $d\Sigma/d\Omega(Q)$
- USAXS imaging

UNICAT Standard USAXS Setup

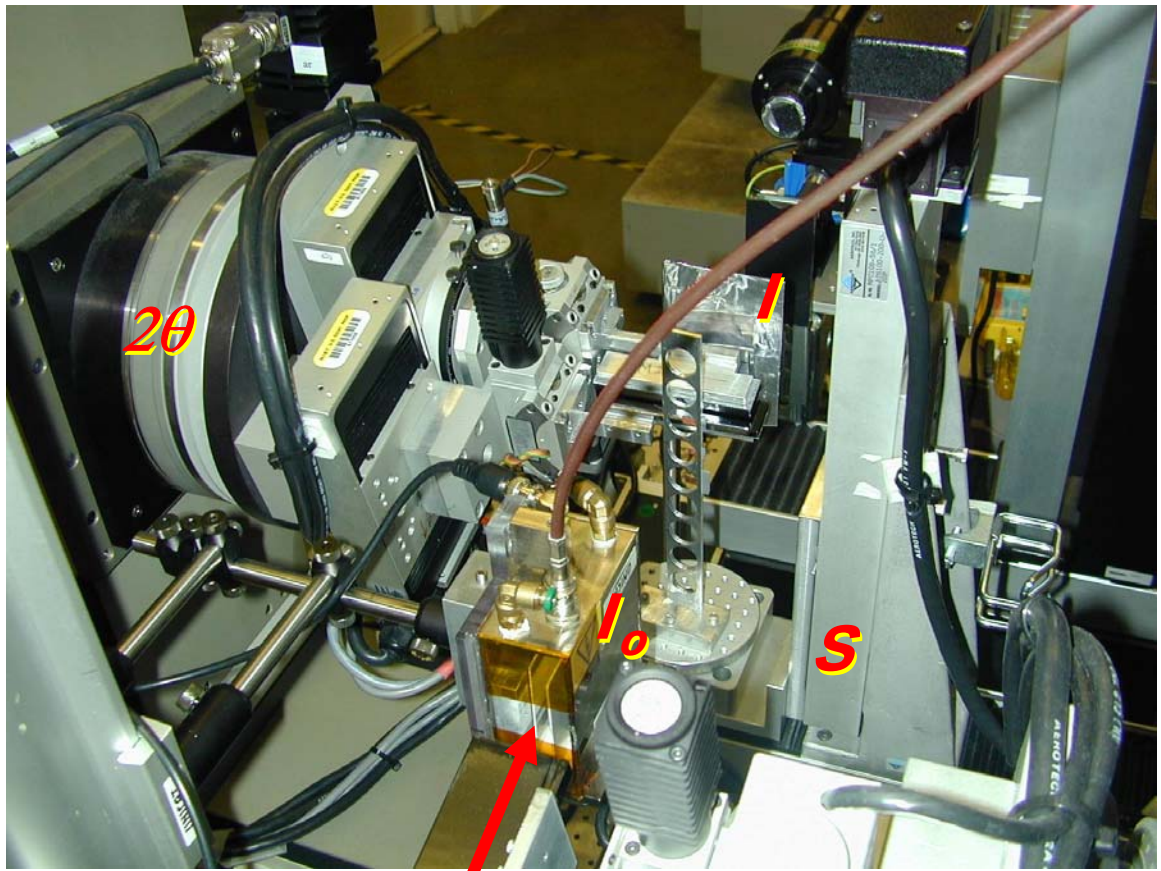

UNICAT USAXS Instrumentation

- Bonse-Hart camera
  - Tested range of energies: 7 – 19 keV (10 keV common)
  - $I_0 > 10^{12}$ ph/s (10 keV) delivered to sample
  - Usual Q range: 0.0002 to 0.1 Å^{-1}
    (very strong scatterers can be measured to 0.8 – 1.0 Å^{-1})
  - Calibration method: direct absolute intensity scaling
    (standard-less method uses known sample thickness, instrument geometry and direct measure of straight-through beam)
  - Detectors:
    - Data: Unbiased PIN Photodiode + linear current amplifier
      50 fA – 1 mA distributed across 5 gain ranges
    - Monitor: Air ion chamber
    - Apparent noise level is about 0.5% of signal
  - Data collection time: ~15 – 20 minutes for 150 points

UNICAT USAXS Geometry Comparison

Comparison of 1-D and 2-D collimation geometries		
	standard USAXS	**2-D collimated SRUSAXS**
collimation	1-D	2-D
desmearing	needed	not needed
Studies	isotropic scatterers	colloids, anisotropic scatterers
Q range	0.00012 $Å^{-1}$ to 1 $Å^{-1}$	0.00012 $Å^{-1}$ to 0.1 $Å^{-1}$
Intensity range	up to 9 decades, $I_0>10^{12}$ ph/s	up to 8 decades , $I_0>10^{11}$ ph/s
Maximum beam size	2.5 mm (h) × 0.4 mm (v)	1.0 mm (h) × 0.4 mm (v)

UNICAT USAXS User support

- Experiment data acquisition in **spec**
  (run from Linux command line)
  - Custom macro package
- Data processing and evaluation in IgorPro
  (run from Windows or Macintosh)
  - Data reduction package: Indra (ver. 2)
  - Data evaluation package: Irena (ver. 1 beta)
  - Both are available: http://www.uni.aps.anl.gov/usaxs

Outline

- Small-Angle Scattering Primer
- Quantitative Small-Angle Scattering
- Instrumentation
- Examples
  - Polystyrene spheres
  - Colloidal silica with ZrO_2 additive
  - Microporous SiO2
  - PMMA bone cement
  - A-USAXS of commercial modified Fe9Cr1Mo steel
  - A-USAXS of commercial silicon nitride
- Summary

Polystyrene spheres:
Determination of Size & Polydispersity

Jemian, Ph.D. Thesis, 1990, Northwestern

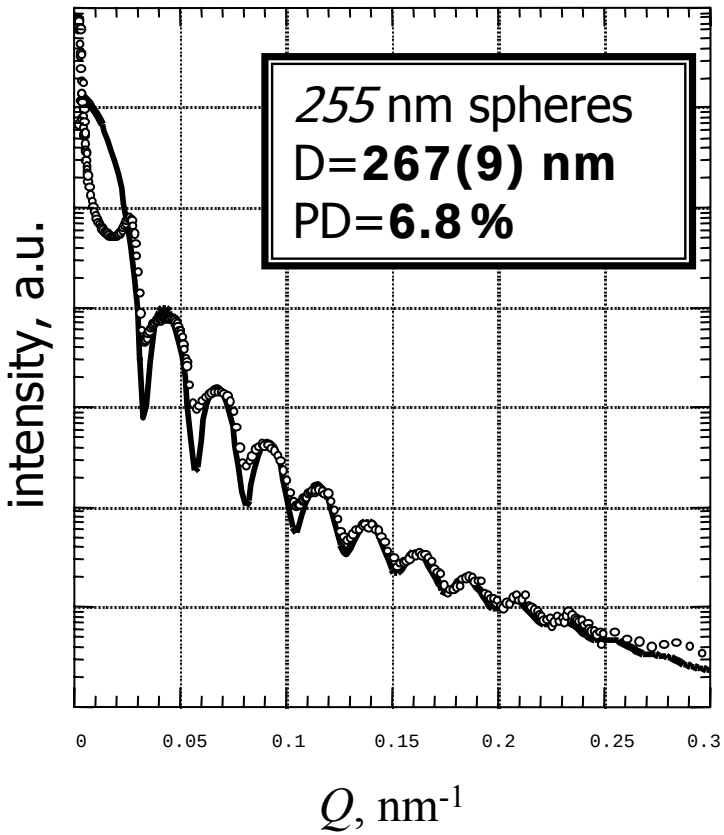

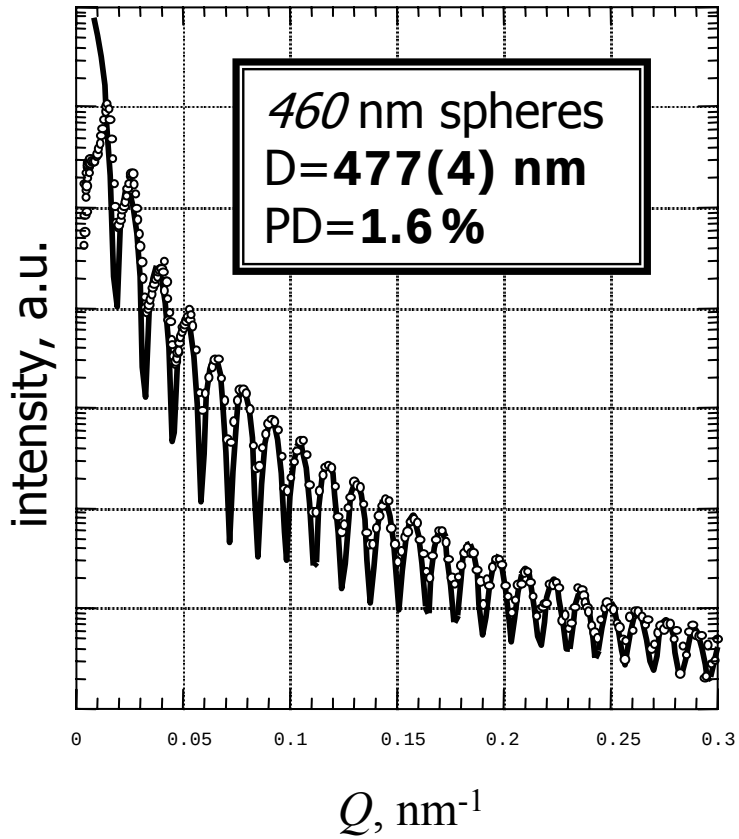

Colloidal silica with zirconia additive

- Nonadsorbing (depletant) zirconia colloids added to disperse silica colloids
- SAS can be used to characterize these sizes

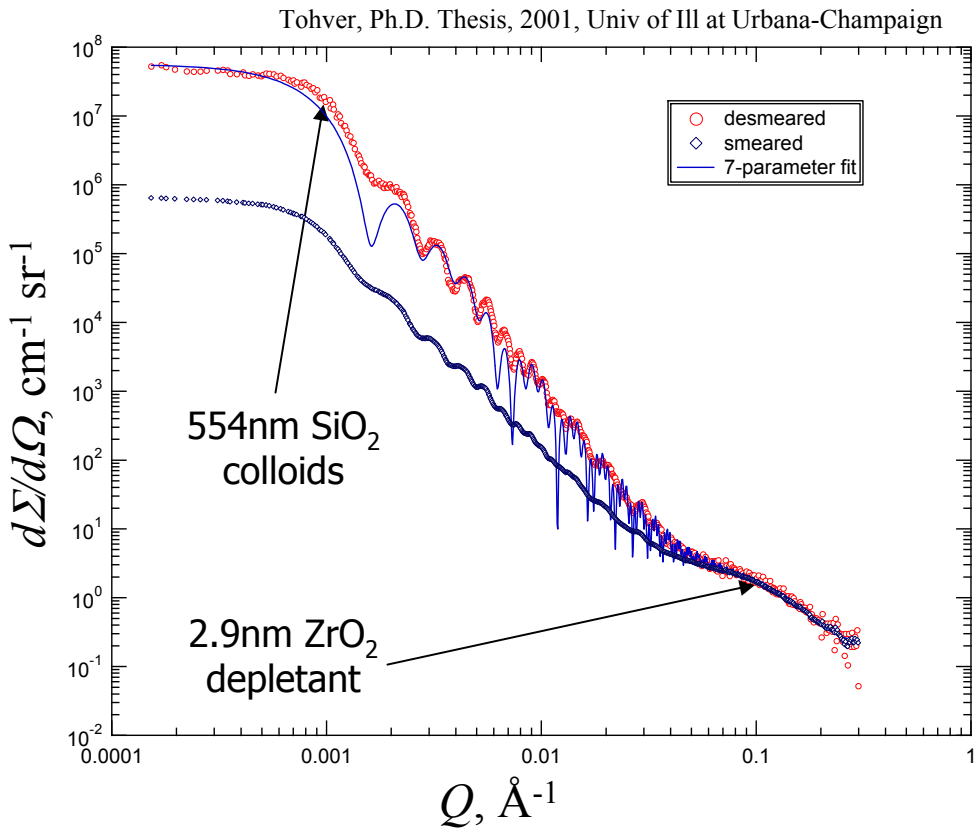

Depletion restabilization of 0.5μm colloidal silica

scattering from each component

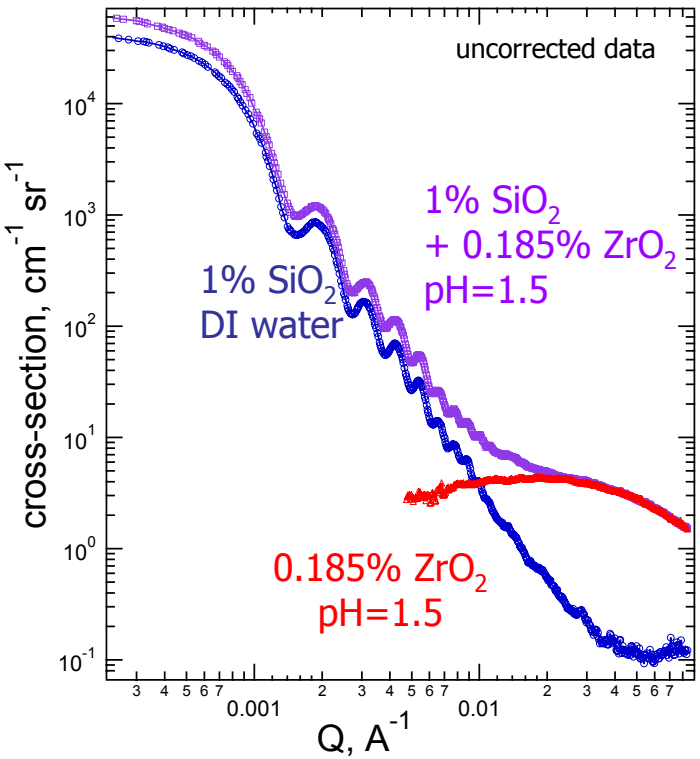

depletant stabilizes suspension

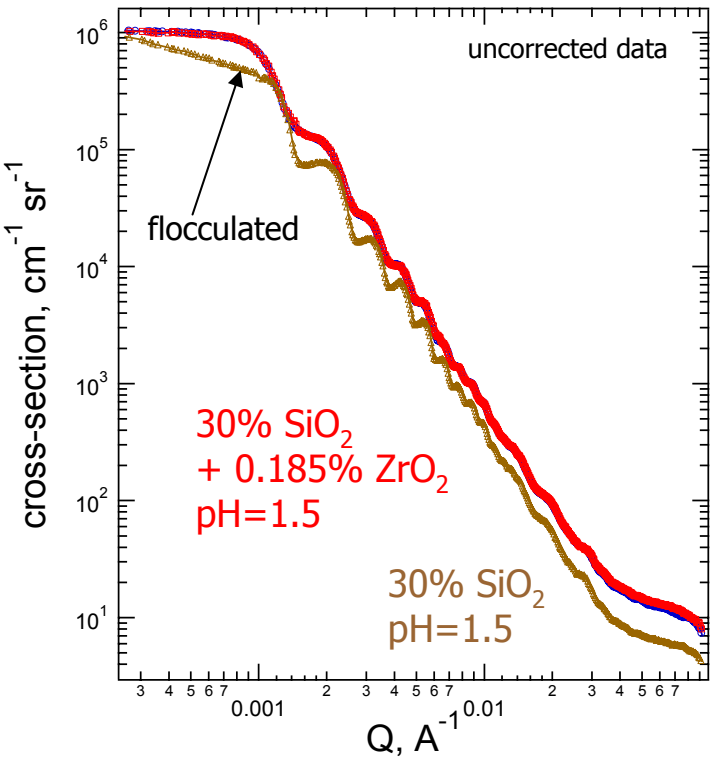

Tohver, private communications, 2000

Porous silica precursor bodies

Long, et al., *J Appl Cryst* **23**.6 (1990) 535

- Prepared by sol-gel process
- Mixtures of colloidal silica and potassium silicate
- Microstructure: array of particles, small clusters, and aggregates of colloids
- USAXS and SANS to characterize polydisperse size distributions of particles in porous medium as function of mixture ratio

Microporous silica results

USAXS data

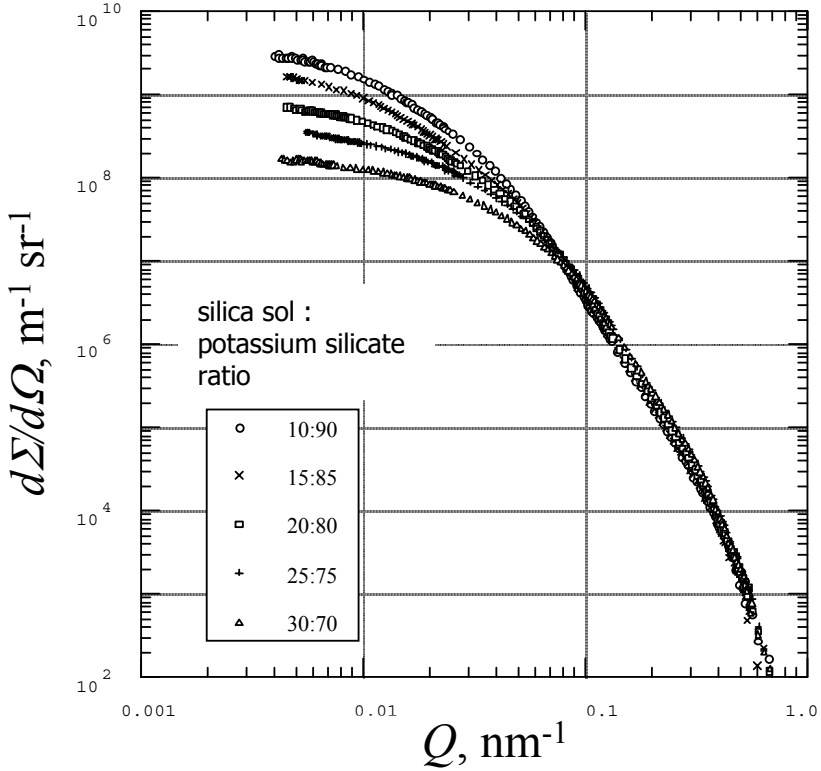

particle size distributions
obtained from USAXS data

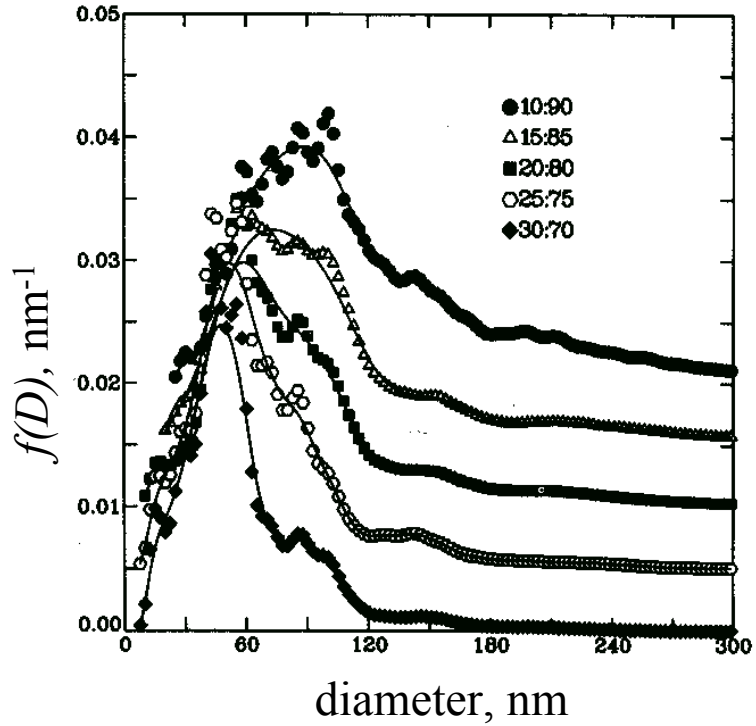

Long, et al., *J Appl Cryst* **23**.6 (1990) 535

Fracture Toughness of PMMA Bone Cement Containing Particulate Fillers

Anuj Bellare, PhD, Wolfgang Fitz, MD, Andreas Gomoll, MD, Richard D. Scott, MD, Thomas S. Thornhill, MD,
Department of Orthopedic Surgery, Brigham and Women's Hospital, Harvard Medical School, Boston, MA

Total Knee and Hip Replacement Prostheses

Barium Sulfate Particulate added to PMMA as Radiopacifier

Bellare, private communications

Radiopacifier Weakens the Bone Cement

Various Bone Cements	Impact Strength (J)
Simplex	0.333± 0.02
Palacos R	0.402± 0.03
Palacos K	0.382± 0.03
CMW – 0	**0.578**± 0.06
CMW+4% $BaSO_4$	**0.323**± 0.03
CMW+8% $BaSO_4$	**0.274**± 0.03
CMW+4.2% Erythocyne	0.461± 0.03
CMW+8% BaSO4+4.2%Ery	0.372± 0.03

de Wijn et al, Acta Orthop Scand, 1975

agglomeration

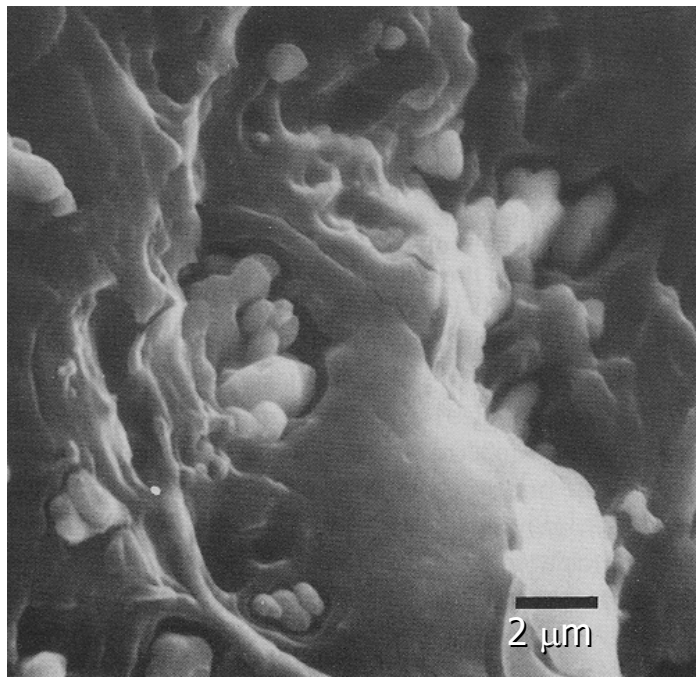

Topoleski et al, J. Biomed Mater. Res., 1990

Nanocomposite Bone Cement

Gomoll, et al., MRS, Vol. 581, (2000) 399

Improved dispersion using nanoscale particulate and surfactant while maintaining radiopacity

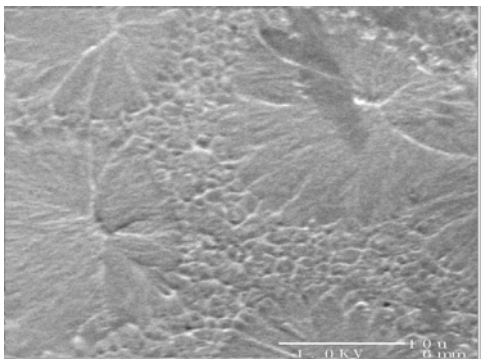

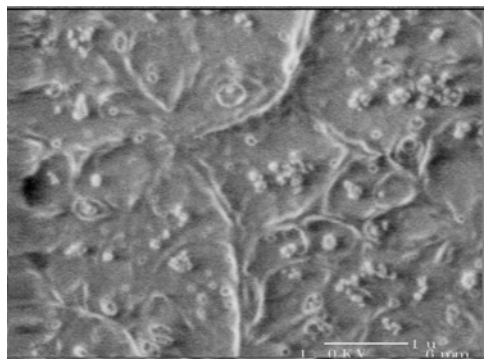

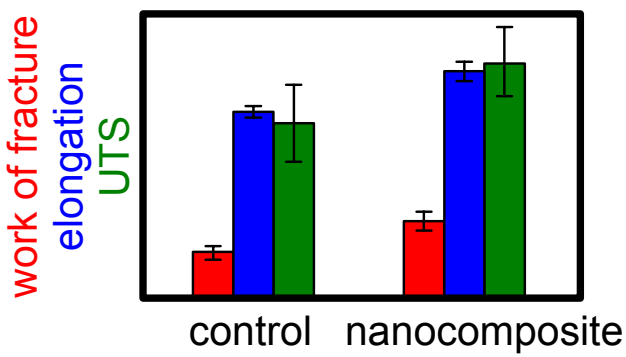

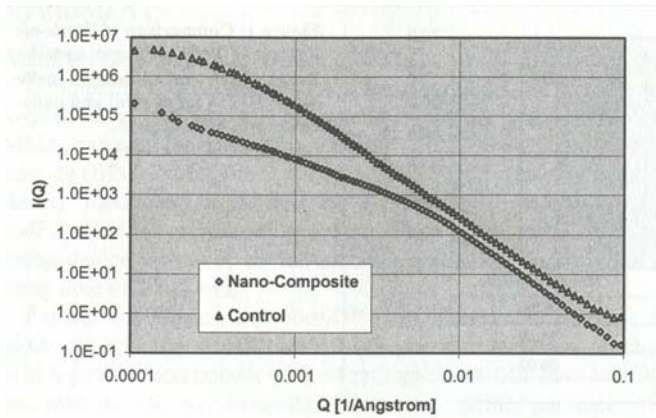

Examples

Hey!
I got one!
I got one!

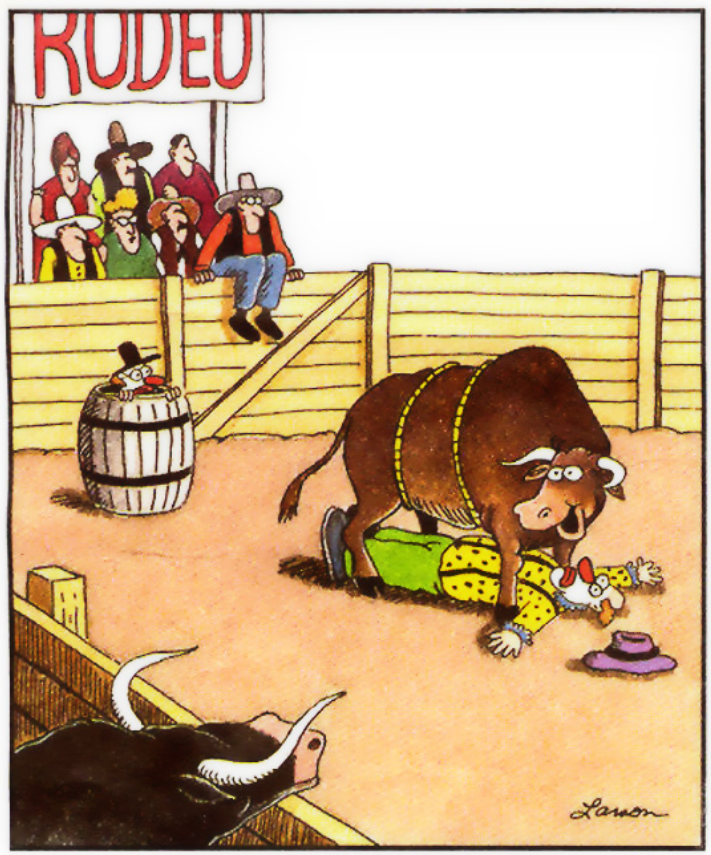

"Hey! I got one! I got one!"

Gary Larson, *The Far Side*

Stability of Modified Fe9Cr1Mo Steel at High Service Temperatures

- Ferritic steel developed at ORNL (1983), proposed for use in power-generation at elevated temperatures
- Attractive properties
  - High temperature use in corrosive environments
  - high rupture strength at both room and elevated temperatures
  - good weldability
  - low thermal expansion
  - resistance to radiation-induced void swelling
- $Cr_{23}C_6$, VC, and NbC present

Chromium Carbide Distribution in Modified Fe9Cr1Mo steel by ASAXS

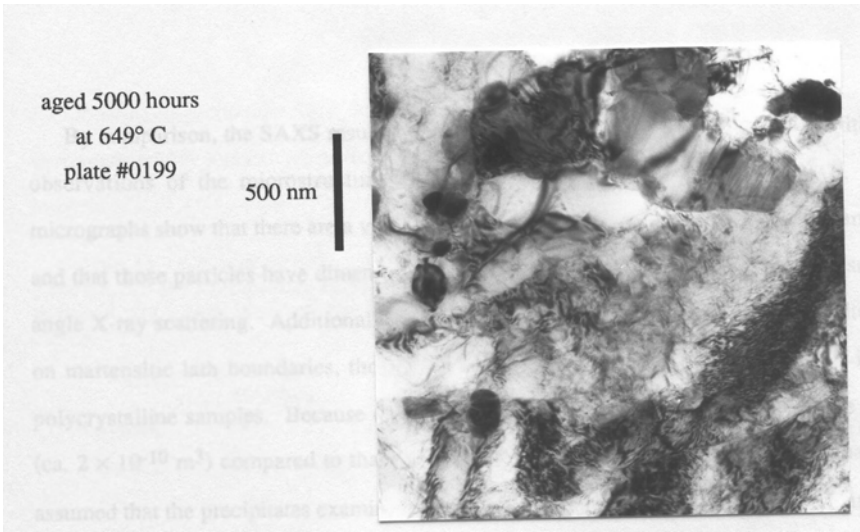

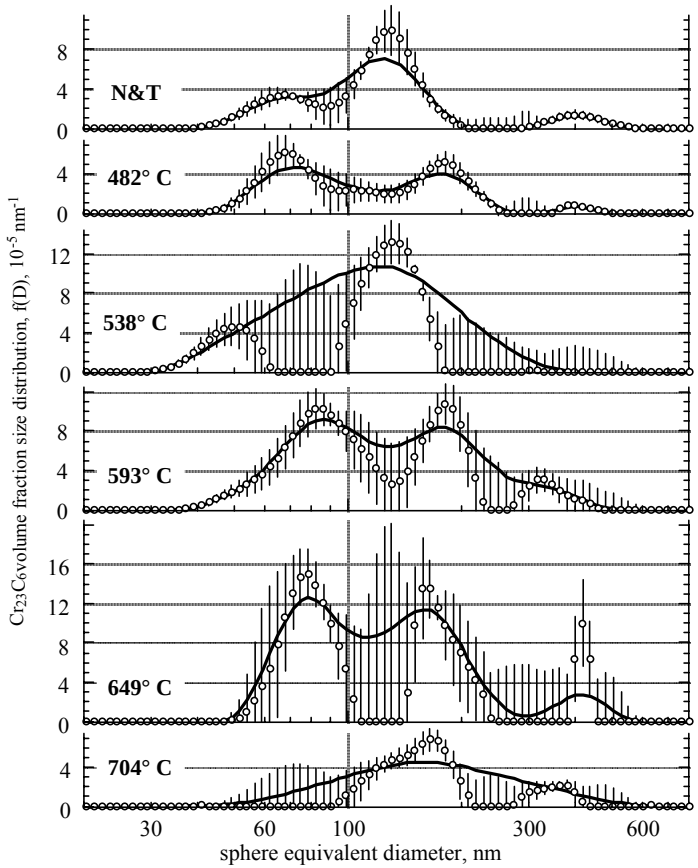

Volume-fraction size distributions of $Cr_{23}C_6$ in Modified Fe9Cr1Mo steel, determined by the ASAXS gradient method. The vertical bars represent the margin of error. The solid line is spline smoothed.

Jemian, Ph.D. Thesis, 1990,Northwestern

Tensile Creep Resistance of Commercial Silicon Nitride

- Prime candidate for structural components in advance gas turbines at high turbine inlet temperatures
- Creep compromises excellent high-temperature mechanical properties
- Cavitation possibly most important mechanism resulting in creep deformation
- Evolution of secondary phase pockets not previously studied due to lack of suitable technique
- Earlier USAXS showed deformation occurs via cavity accumulation at multigrain junctions
- Follow evolution of Yb-rich secondary phase pockets and voids as a function of creep testing using A-USAXS

Silicon Nitride Microstructure

–commercial grade of gas-pressure sintered silicon nitride (designated SN88)

– β-Si_3N_4 grains

–major crystalline secondary phase after heat treatment is ytterbium disilicate, $Yb_2Si_2O_7$

–minor phases include residual $Yb_4Si_2N_2O_7$, $Y_5Si_3NO_{12}$, residual SiO_2 glass, and porosity

Tensile Creep Resistance of Commercial Silicon Nitride

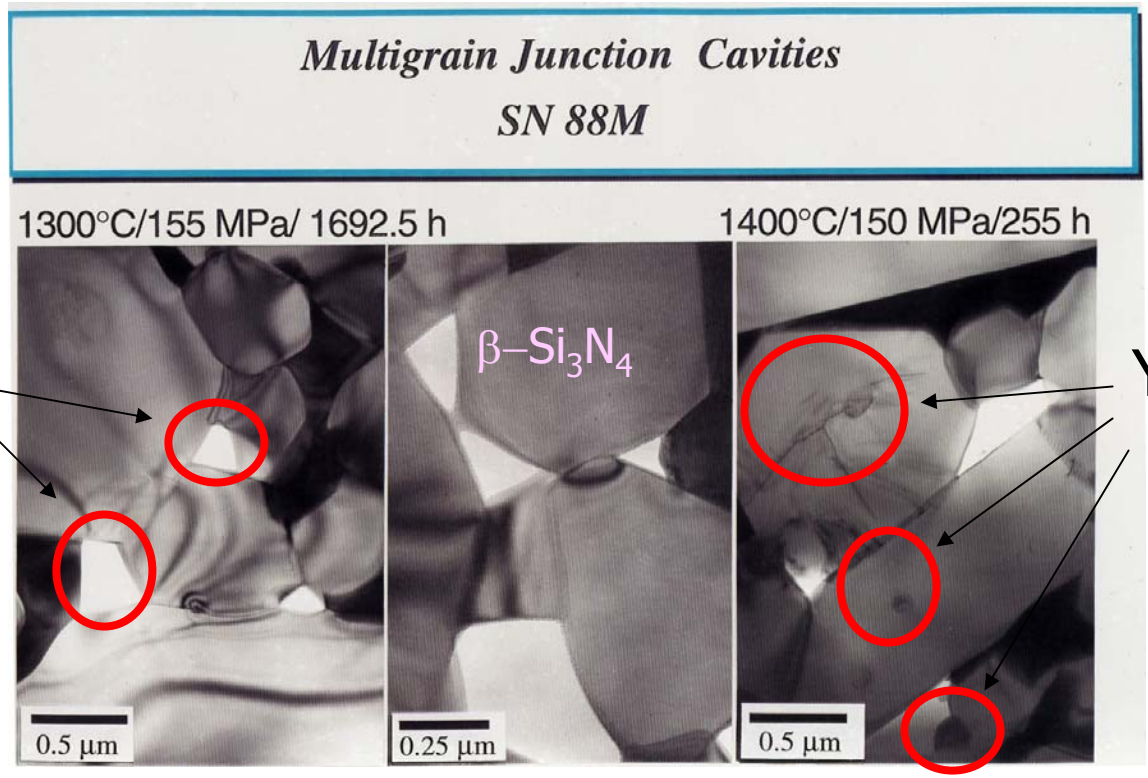

- commercial grade of gas-pressure sintered silicon nitride (designated SN88)
- β-Si_3N_4 grains
- major crystalline secondary phase after heat treatment is ytterbium disilicate, $Yb_2Si_2O_7$
- minor phases include residual $Yb_4Si_2N_2O_7$, $Y_5Si_3NO_{12}$, residual SiO_2 glass, and porosity

Silicon nitride SN-88 samples

- Five tensile creep tests
- Different test times: 30 s – 85 h
- 1400° C, 150 MPa load
- Tests interrupted and cooled under load
- A-USAXS samples ground and hand-polished
- Sample from undeformed grip, 180 μm
- Sample from gage parallel to stress axis, 100 μm

A-USAXS near the Yb L_{III} edge from SN-88 tensile creep sample, 50 h

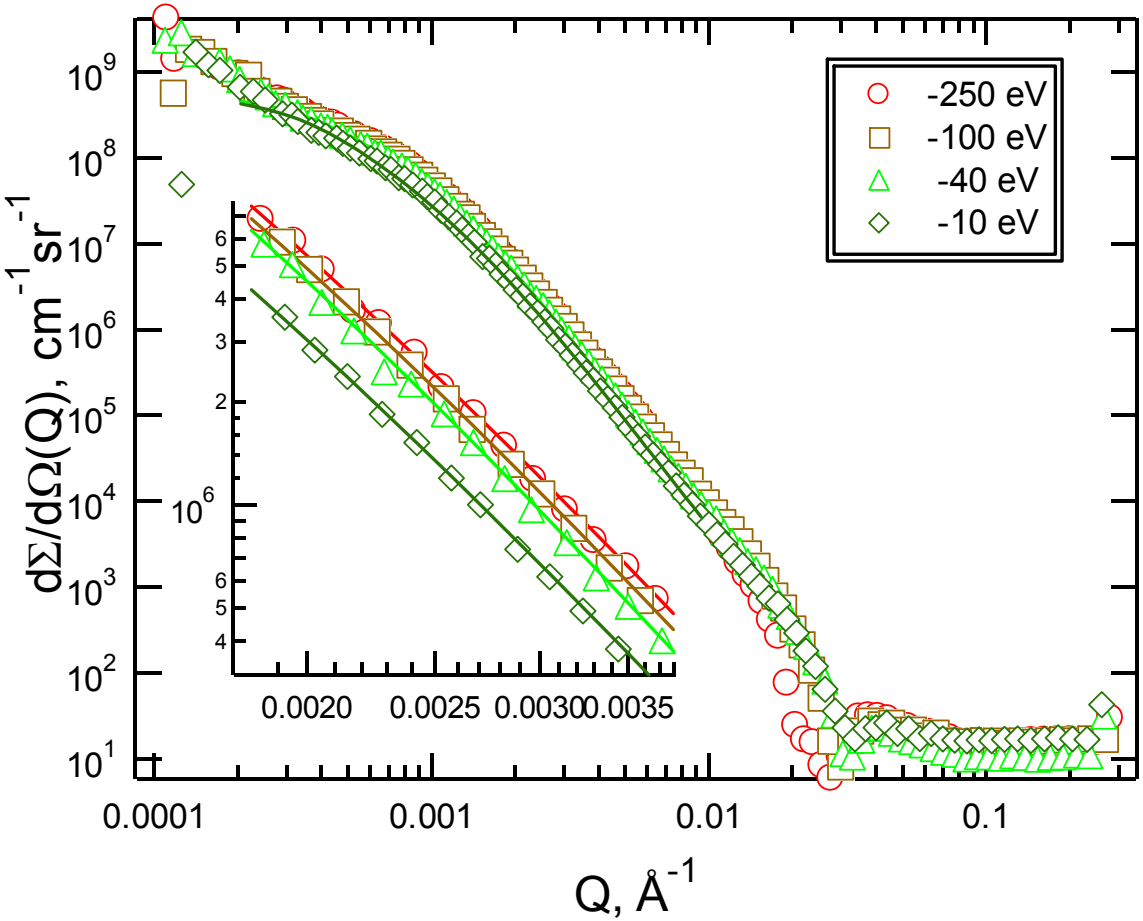

A-USAXS size distributions from SN-88 near the Yb L_{III} edge

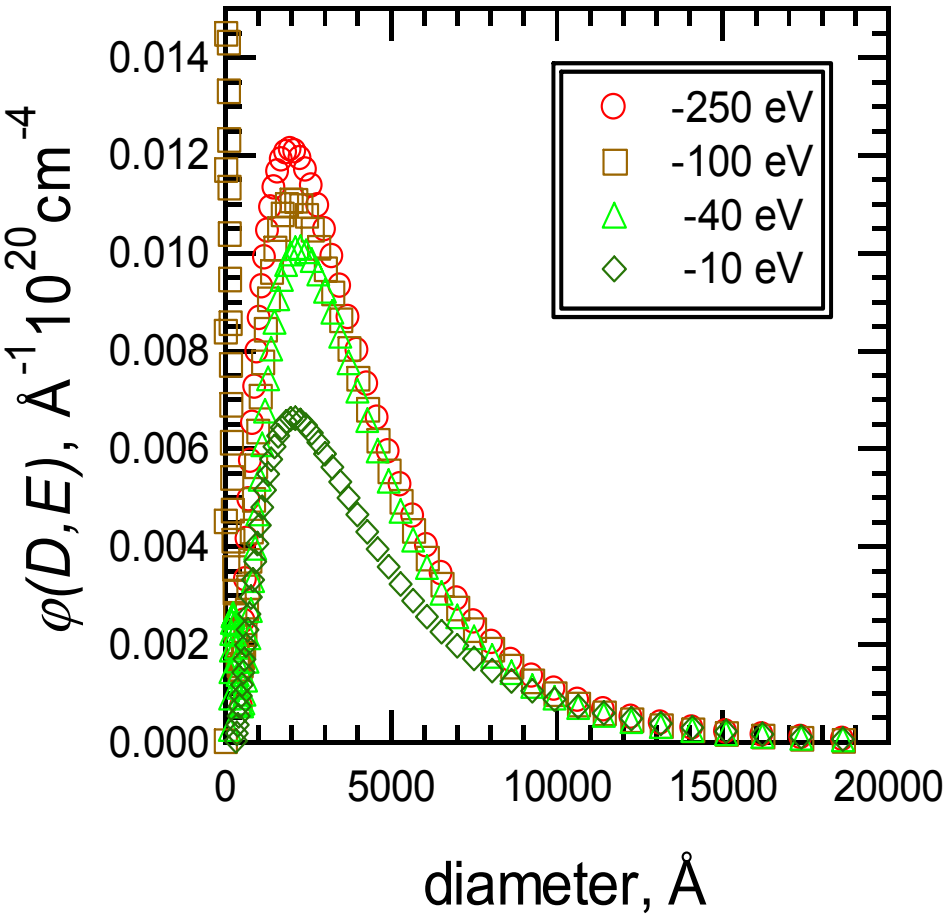

Yb disilicate and tensile creep cavity size distributions from SN-88

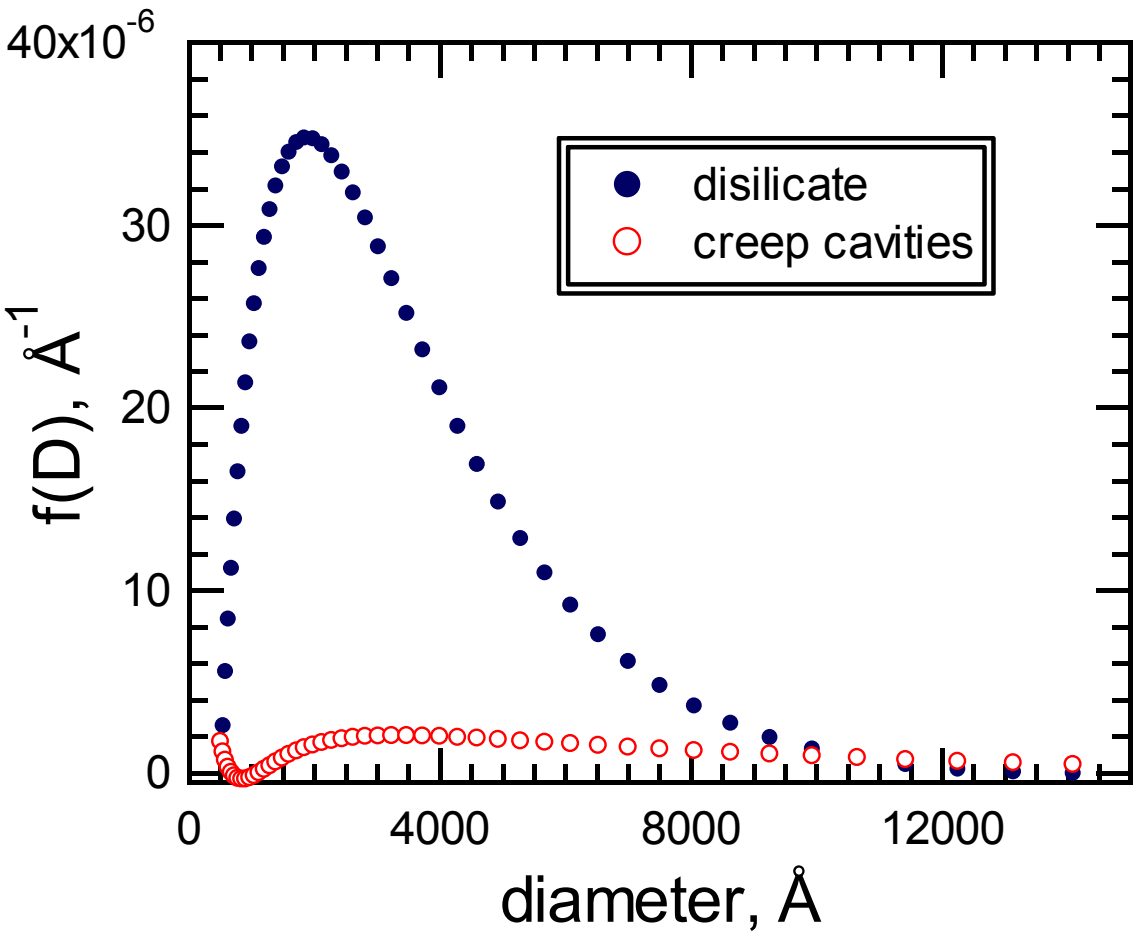

Evolution of size distributions in SN-88 with test time, 1400 C

Yb disilicate size distributions, grip section

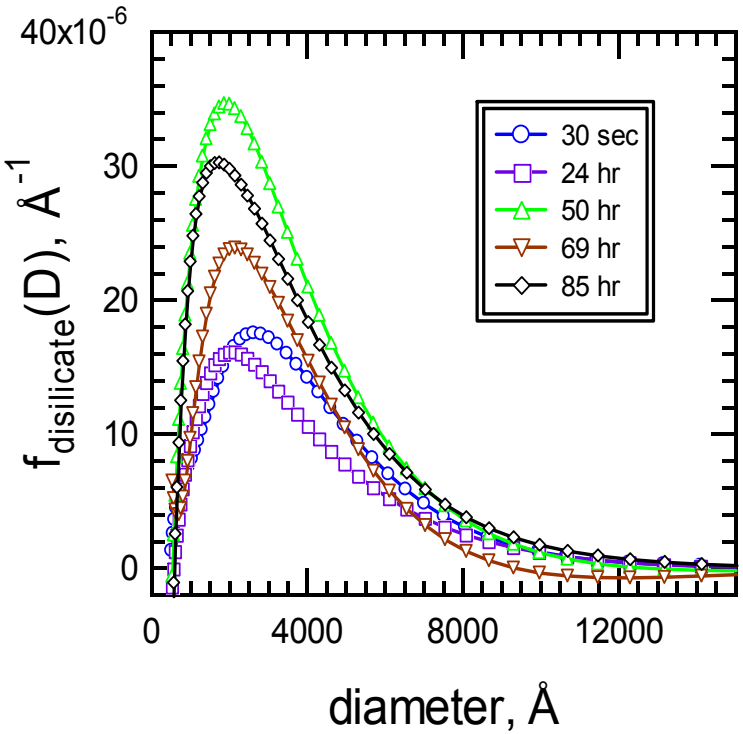

tensile creep cavity size distributions

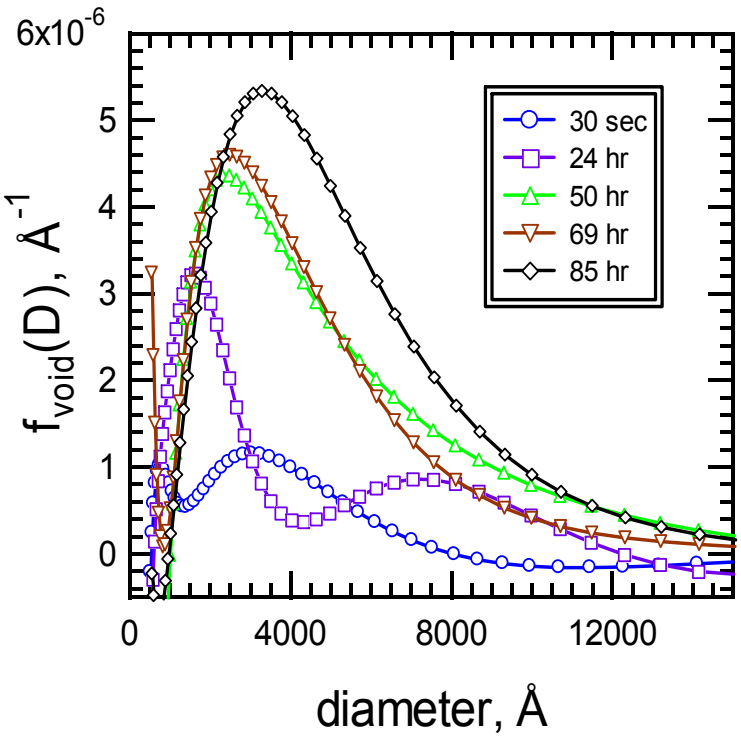

Creep strain and cavitation in SN-88

J. Eur. Ceram. Soc. 22 [14-15] 2479-2487 (2002).

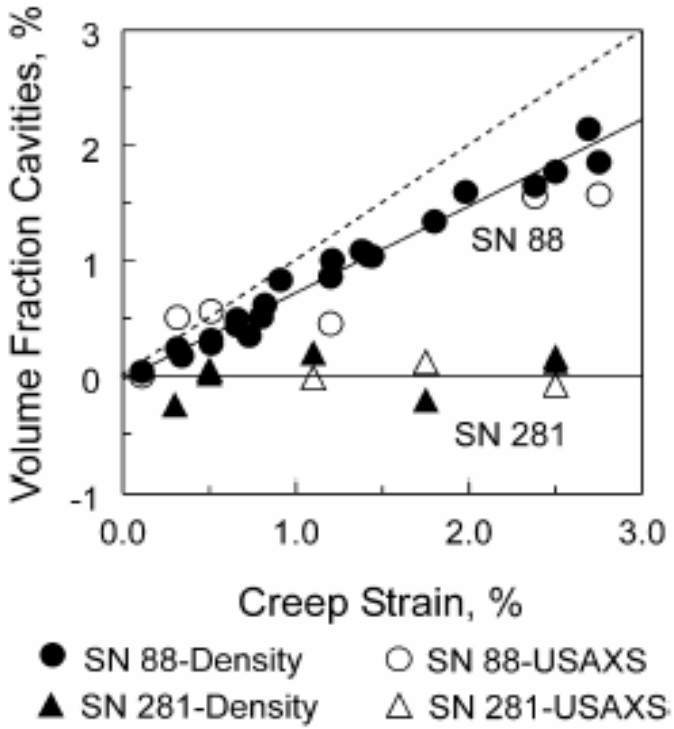

Fig. 6. A comparison of the dependencies between strain and volume fraction of cavities determined from USAXS and density change measurements in SN 281 and SN 88.[16,30] The contribution of cavities to tensile strain in SN 281 is close to zero while it is around 70% in SN 88.

Tensile Creep Resistance of Commercial Silicon Nitride: A-USAXS Results

Lofaj, Wiederhorn, Long, Hockey, Jemian, Browder, Andreasen, & Taffner;
***J Euro Ceram Soc* 22** (2002) 2479-2487.

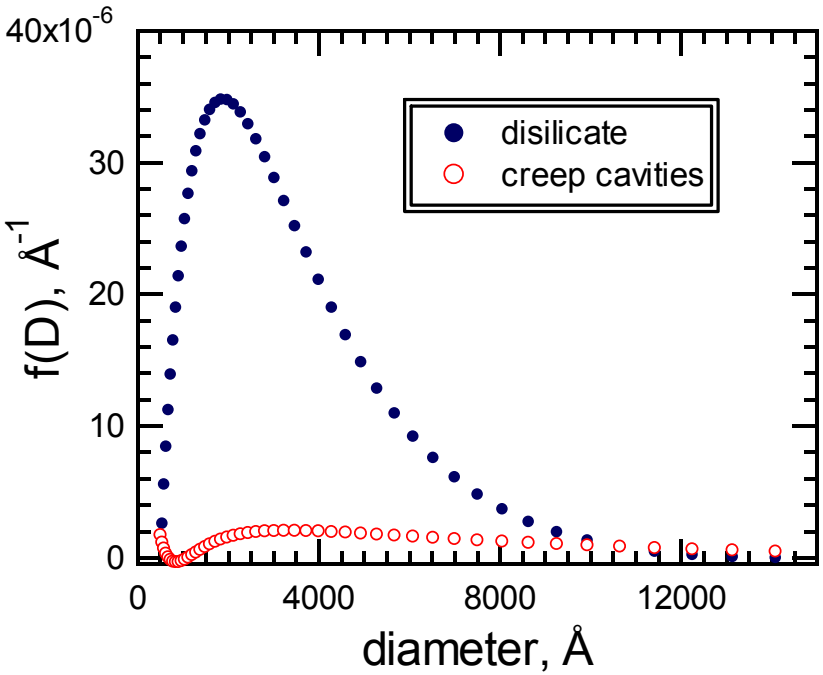

Creep pore size distribution separated from size dist of secondary phase pockets of comparable size.

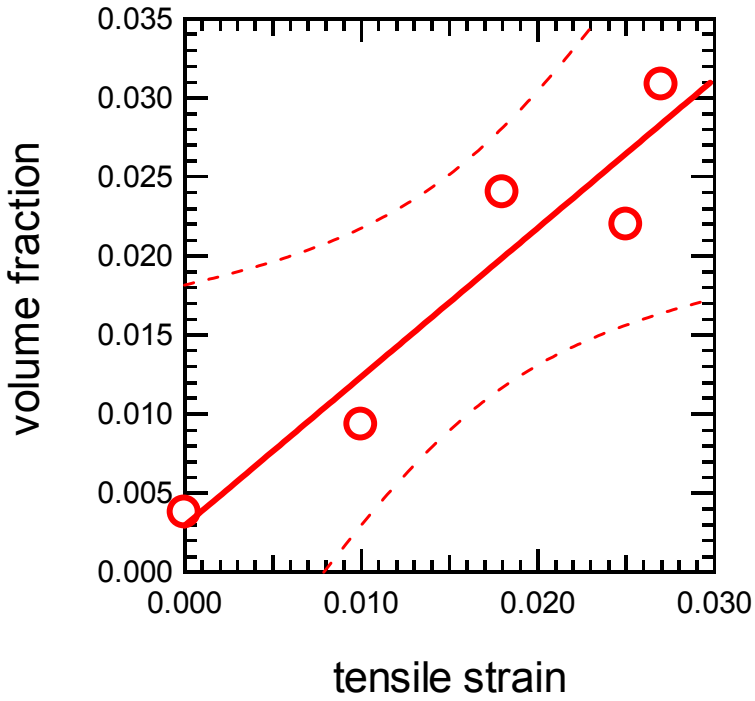

Linear relationship between *Vv* measured from A-USAXS and tensile strain agrees well with density change data and confirms that cavitation is the main creep mechanism.

Conclusions: SN88 A-USAXS study

- A-USAXS used to determine simultaneously Yb disilicate and creep cavity size distributions in SN-88
- Yb disilicate and creep cavities were of comparable size
- V_v of Yb disilicate 5-8 times greater than V_v of creep cavities
- V_v of creep cavities proportional to tensile strain, slope = 1
- Good agreement with density change data
- Confirmation that cavitation is the main creep mechanism
- A-USAXS obtained statistically-significant measurements of Yb-rich secondary phase pockets during creep in the presence of a creep cavity population of similar dimensions

Outline

- Small-Angle Scattering Primer
- Quantitative Small-Angle Scattering
- Instrumentation
- Examples
- Summary

Wrap up

- SAS investigations measure nanoscale microstructure
- Many different materials of technological importance can be investigated
- Contrast variation methods possible
- Statistically significant results
- Unique results not obtainable by other methods
- Complementary methods increase the information content which can be realized from a quantitative SAS investigation

Resources

- Organizations
  - IUCr SAS http://www.iucr.org/iucr-top/iucr/csas.html
  - ANL SAS SIG http://small-angle.anl.gov
  - UNICAT USAXS http://www.uni.aps.anl.gov

- References
  - *Small-Angle Scattering of X-rays*, André Guinier and Gérard Fournet, John Wiley & Sons, New York, 1955
  - *Small-Angle X-ray Scattering*, H. Brumberger, Gordon and Breach, Syracuse University, 1965
  - *Small-Angle X-ray Scattering*, Otto Glatter and O. Kratky, Academic Press, London, 1982
  - *Neutron, X-ray and Light Scattering: Introduction to an Investigative Tool for Colloidal and Polymeric Systems*, European Workshop on Neutron, X-ray and Light Scattering as an Investigative Tool for Colloidal and Polymeric Systems, edited by Peter Lindner and Thomas Zemb, Bombannes, France, 1990 (North-Holland, Amsterdam)
  - *Modern Aspects of Small-Angle Scattering*, NATO Advanced Study Institute on Modern Aspects of Small-Angle Scattering, Vol. C451, edited by Harry Brumberger, Como, Italy, 1993 (Kluwer Academic Publishers, Dordrecht)

Collaborators

- *Brigham and Women's Hospital, Harvard Medical School*
  Anuj Bellare
- *Georgia Institute of Technology*
  Rosario Gerhardt, Yongwen Yuan
- *NIST*
  Gabrielle G. Long, Andrew J. Allen, Jan Ilavsky, Sheldon M. Wiederhorn, Frank Lofaj
- *Northwestern University*
  Julia Weertman
- *UNICAT, Advanced Photon Source*
  Paul Zschack, Hawoong Hong, Jenia Karapetrova
- *University of Illinois at Urbana-Champaign*
  Charles F. Zukoski, Jennifer Lewis, Valeria Tohver, Syed Ali Shah, Subramanian Ramakrishnan